International Journal of
*Environmental Research and Public Health*

MDPI

*Article*

# Epidemiology of Δ8THC-Related Carcinogenesis in USA: A Panel Regression and Causal Inferential Study

**Albert Stuart Reece [1,2,*] and Gary Kenneth Hulse [1,2]**

[1] Division of Psychiatry, University of Western Australia, Crawley, WA 6009, Australia; gary.hulse@uwa.edu.au
[2] School of Medical and Health Sciences, Edith Cowan University, Joondalup, WA 6027, Australia
* Correspondence: stuart.reece@bigpond.com; Tel.: +617-3844-4000; Fax: +617-3844-4015

**Abstract:** The use of Δ8THC is increasing at present across the USA in association with widespread cannabis legalization and the common notion that it is "legal weed". As genotoxic actions have been described for many cannabinoids, we studied the cancer epidemiology of Δ8THC. Data on 34 cancer types was from the Centers for Disease Control Atlanta Georgia, substance abuse data from the Substance Abuse and Mental Health Services Administration, ethnicity and income data from the U.S. Census Bureau, and cannabinoid concentration data from the Drug Enforcement Agency, were combined and processed in R. Eight cancers (corpus uteri, liver, gastric cardia, breast and post-menopausal breast, anorectum, pancreas, and thyroid) were related to Δ8THC exposure on bivariate testing, and 18 (additionally, stomach, Hodgkins, and Non-Hodgkins lymphomas, ovary, cervix uteri, gall bladder, oropharynx, bladder, lung, esophagus, colorectal cancer, and all cancers (excluding non-melanoma skin cancer)) demonstrated positive average marginal effects on fully adjusted inverse probability weighted interactive panel regression. Many minimum E-Values (mEVs) were infinite. *p*-values rose from $8.04 \times 10^{-78}$. Marginal effect calculations revealed that 18 Δ8THC-related cancers are predicted to lead to a further 8.58 cases/100,000 compared to 7.93 for alcoholism and −8.48 for tobacco. Results indicate that between 8 and 20/34 cancer types were associated with Δ8THC exposure, with very high effect sizes (mEVs) and marginal effects after adjustment exceeding tobacco and alcohol, fulfilling the epidemiological criteria of causality and suggesting a cannabinoid class effect. The inclusion of pediatric leukemias and testicular cancer herein demonstrates heritable malignant teratogenesis.

**Keywords:** cannabis; cannabinoid; Δ8THC; teratogenesis; oncogenesis; carcinogenesis; cancer; cancerogenesis



**Citation:** Reece, A.S.; Hulse, G.K. Epidemiology of Δ8THC-Related Carcinogenesis in USA: A Panel Regression and Causal Inferential Study. *Int. J. Environ. Res. Public Health* **2022**, *19*, 7726. https://doi.org/10.3390/ijerph19137726

Academic Editor: Paul B. Tchounwou

Received: 19 April 2022
Accepted: 21 June 2022
Published: 23 June 2022



## 1. Introduction

Δ8THC use and exposure is increasingly dramatically in many parts of the USA driven partly by the rubric of being "legal weed" [1]. Δ8THC differs from Δ9THC chemically by having the double bond on the eighth carbon on the C-ring whereas in Δ9THC, the double bond is on the ninth [2]. Δ8THC differs from Δ9THC biologically as its effects are milder than those of Δ9THC [2] notwithstanding, for which recent warnings concerning adverse effects have recently been issued from both the Centers for Disease Control (CDC) Atlanta, Georgia and the Food and Drug Administration (FDA) [3,4]. Like Δ9THC, Δ8THC is a partial agonist at CB1 receptors (CB1R) [2,5]. Its effects in overdose seem to closely parallel those of Δ9THC including sedation, nausea, vomiting, dysphoria, and hallucinations [2,6].

Several cannabinoids also have a long history as known genotoxic compounds. This has been demonstrated in the laboratory with toxic effects on chromosomes [7–12], DNA strands [13], DNA nucleoside bases [13], the epigenome [14–16], and intermediary metabolism, which drive epigenomic processes [17–21], being well-described. The adult cancer most strongly implicated with cannabis exposure is testicular cancer [22–25], but several childhood cancers including acute myeloid leukemia, rhabdomyosarcoma, and neuroblastoma

have also been described in association with cannabis exposure [26]. Further interest in this issue has recently been aroused with the description that breast cancer, the most common cancer in many countries, is linked with cannabis exposure, along with thyroid, liver, and pancreatic tumors and acute myeloid leukemia [27]. Moreover, cannabis exposure has also been linked with the most common childhood cancer, acute lymphoid leukemia [28], and cannabis has also been shown to be a primary driver of total childhood cancer [28]. Since childhood cancers generally arise as a result of inherited genotoxic damage [29,30], such findings necessarily raise the concern of mutagenic processes with intergenerational impacts.

Like other cannabinoids [31–35], Δ8THC has also been shown to inhibit DNA synthesis [5,36–39]. Indeed, in one relative potency study, Δ8THC was shown to inhibit DNA synthesis more strongly and for a longer duration than other cannabinoids including Δ9THC [38]. Whilst this suggests an anti-cancer action for Δ8THC derivatives [36,37,39,40], its effects in vivo may be to potentiate carcinogenesis by interfering with DNA, RNA, and key nucleoprotein metabolism and DNA maintenance pathways [37,38]. As it has been shown long ago that the genotoxic moiety of cannabinoids resides in their central olevitol nucleus core structure [41,42], it is entirely possible that the described genotoxicity of many cannabinoids [13,43] is actually a class effect pertaining broadly to numerous cannabinoid derivates.

As important as malignant outcomes are, recent reports indicate that the stakes are likely much higher, even than cancer. Cannabinoids have recently been linked with numerous severe congenital anomalies [27,44–47]. Moreover, recent studies have confirmed that epigenotoxicity causally mediates the aging processes [48]. Such findings greatly extend the present concerns relating to genotoxicity horizontally throughout the community via food chain contamination and vertically with transgenerational temporality.

As the issue of the potential relationship of Δ8THC to cancer presently represents a knowledge gap, we sought to investigate relevant epidemiological evidence in the USA using the most recent data available. Our hypothesis of a potential relationship between Δ8THC and cancer was formulated prior to commencement of the study.

## 2. Methods

Data. Age adjusted cancer incidence data were accessed from the Surveillance Epidemiology and End Results (SEER) database held by the National Cancer Institute and the Centers for Disease Control (CDC) Atlanta Georgia using the SEER*Stat software from CDC [49]. State-level drug use prevalence data were accessed from the Substance Abuse and Mental Health Services Administration (SAMHSA) Restricted Data Access Scheme (RDAS) of the annual National Survey of Drug Use and Health (NSDUH), a large nationally representative survey with a 74.1% response rate [50]. Substances of interest were cigarettes, alcohol abuse or dependency (such as alcohol use disorder, AUD), last month of cannabis use, last year of narcotic analgesic abuse, and last year of cocaine use. Median household income, ethnicity, and population data was from the U.S. Census Bureau using the R Package tidycensus [51]. The ethnicities considered were Caucasian American, African-American, Asian-American, Hispanic-American, American Indian/Alaskan Native American (AIAN), and Native Hawaiian/Pacific Islander American (NHPI). Mean cannabinoid concentration in federal seizures was taken from published reports [52–54].

Derived data. Quintiles of substance exposure were calculated by dividing up the range of substance exposures across the whole period for which data were available. Estimates of state-level cannabinoid exposure were obtained by multiplying the state-level of cannabis use by the concentration of the cannabinoids found in Federal seizures.

Statistics. Data were processed in R Studio (1.4.1717) based on R (4.1.1), both obtained from the comprehensive R Archive Network (CRAN). The analysis was performed in October 2021. Data were manipulated with dplyr and graphs were drawn using ggplot2, both from the tidyverse software suite [55]. Maps were drawn using the R package simple features (sf) [56]. Heatmaps were drawn in gplots [57]. All graphs and graphs are

original. Relative risk ratios (RR), attributable fraction in the exposed (AFE), and population attributable risk (PAR) and their confidence intervals were calculated on the categorical data using the R package epiR [58]. Multivariable panel regression was performed using the R-package plm [59] and allows for data to be considered in its space–time context (using the "twoway" effect), the temporal lagging to be used, and E-Values to be calculated. All panel models were inverse probability weighted using the ipw R package [60]. In all interactive models, a three-way interaction was introduced between tobacco, alcohol use disorder, and Δ8THC exposure. E-values, or expected values, allow for a quantification of the extent to which an observed association might possibly be attributed to external or extraneous uncontrolled covariates [61,62]. E-Values were calculated using the EValue R package [63]. The E-Value has a confidence interval reflecting its upper and lower bound. Minimum E-Values in excess of 1.25 are said to indicate causality [64] and E-Values exceeding nine are considered to be very high [65]. Marginal overall effect sizes for panel models was estimated using the R package margins [66]. All tumor types were considered simultaneously using an iterative analytical approach in purrr (from tidyverse [55]) and the above R Packages together with broom [67].

Data availability. Data have been made publicly available through the Mendeley data repository and can be accessed at this URL doi:10.17632/nhprw35ppb.1.

Ethical approval. Ethical permission for this study was granted through the University of Western Australia Human Research Ethics Committee on 24 September 2021 with HREC Number 2019/RA/4/20/4724.

## 3. Results

As shown in Table S1, 14,598 age-adjusted cancer incidence rates were downloaded from the CDC/NCI SEER database for the years 2009–2017. This time range represents the range for which both cancer and cannabinoid concentration data are available. The 34 cancer types of interest are listed in Table S1. This table also provides data on state-level substance exposure rates together with estimates of state-level cannabinoid exposure and ethnicity and median household income, which were the other input covariates. Time trends of the mean cannabinoid content of USA seizures of cannabis at the Federal level are shown in Figure S1. Most cannabinoids are noted to be rising, with the notable exception of cannabidiol. A map showing the estimates of state-level Δ8THC exposure across USA over time is shown in Figure S2. Figure 1 illustrates a map-graph of the log Δ8THC state-level exposure estimates.

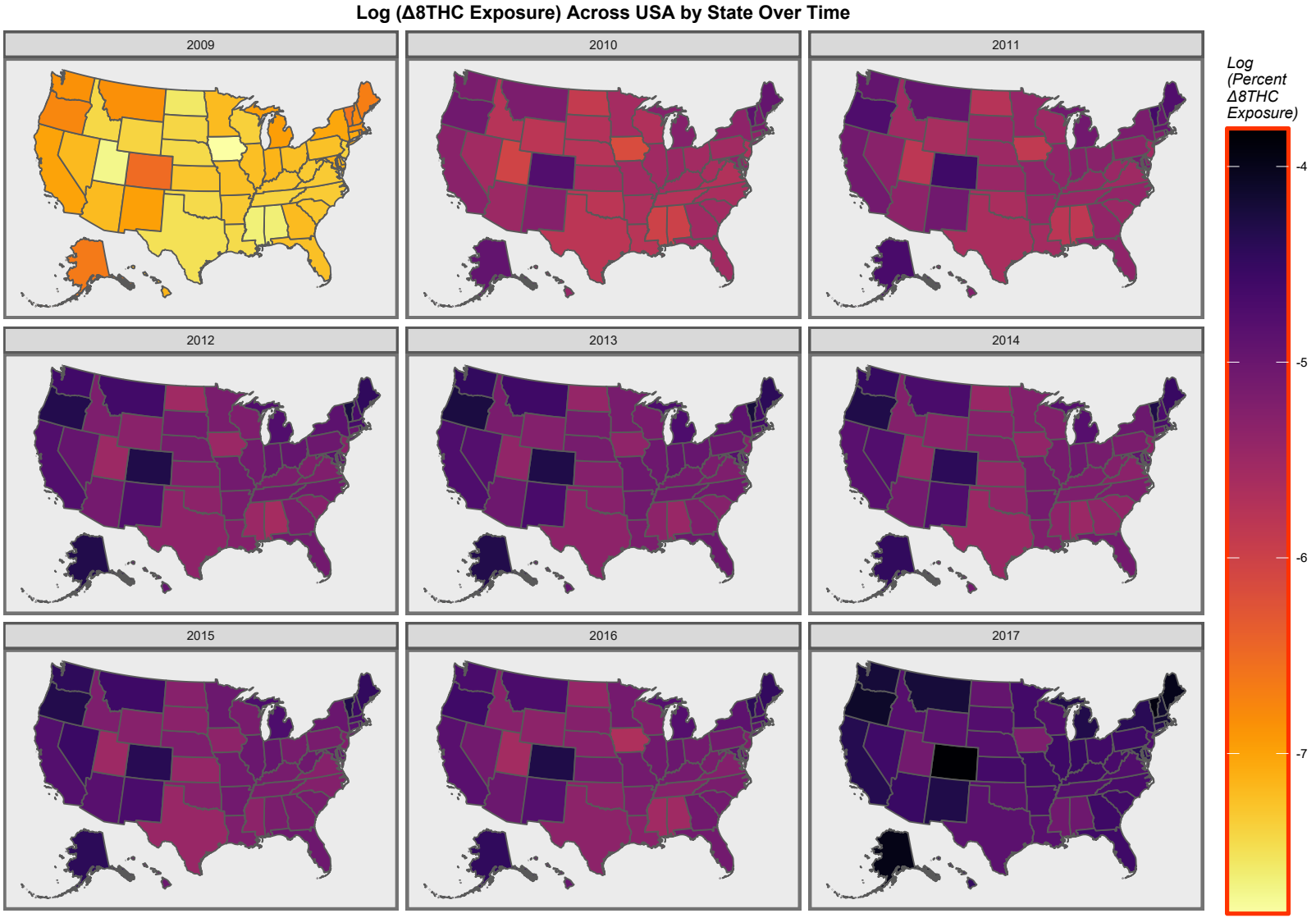


**Figure 1.** Map of the log (Δ8THC estimates) across the USA over time.

### 3.1. Continuous Bivariate Analysis

Figure S3 shows the incidence of the 34 cancers of interest as a gradient function of tobacco exposure. The graph successfully identified many tumors that are known to be tobacco related including lung, larynx, colorectal, cervical, bladder, and all (excluding non-melanoma skin) cancers, etc. Similarly, Figure S4 shows 34 cancer types as a function of alcohol consumption. In this graph, bladder, gastric, post-menopausal breast, and esophageal cancer are all cancers known to be associated with alcohol, which were correctly identified.

Figure S5 illustrates the gradients of these cancers with state-level estimates of Δ9THC exposure. Gastric, post-menopausal breast, breast, bladder, liver corpus uteri, and thyroid cancers were all positively identified, some of which have recently been reported [27]. Figure 2 makes a similar plot for the state-level estimates of Δ8THC exposure. In this graph, the slopes of the associations with cancers of the following sites were all obviously positive: corpus uteri, gastric, breast overall and post-menopausal breast, liver, anorectum, pancreas, and thyroid cancers. A formal analysis of these trend lines is shown in Tables S2–S5, which demonstrates that 16, 11, 8, and 8, cancers had elevated minimum E-Values (mEV) each for tobacco, alcohol, Δ9THC, and Δ8THC, respectively.

### 3.2. Categorical Bivariate Analysis

Figures S6–S9 illustrate the bivariate comparisons of the highest and lowest exposure quintiles for these four substances by tumor type. A formal analysis of this categorical data by cancer and by substance is shown in Tables 1 and S6–S9, which demonstrate that for tobacco, alcohol, Δ9THCm and Δ8THC, 16, 15, 11, and 12 cancer types demonstrated elevated minimum E-Values, respectively.

### 3.3. Multivariable Panel Regression

Having identified that several substances were related to cancer incidence, the next question related to their relative importance. Panel regression allowed for these issues to be considered in their native space–time context. An inverse probability weighted comprehensive additive model including tobacco, alcohol, analgesics, cocaine, Δ8THC exposure, median household income, and all ethnicities was considered. A total of 77 significant terms with positive regression coefficients are shown in Table S9. Table S10 selects the fifteen tumor types with which Δ8THC exposure was positively associated. One notes here that this list is headed by tumors of the ovary, oropharynx, gastric cardia, and post-menopausal breast cancer, which have $p$-values as low as $1.02 \times 10^{-69}$ and minimum E-Values ascending from $2.64 \times 10^{14}$. Table S9 is summarized in Table S11 by covariate. The number of cancers implicated, the negative sum of the $p$-value exponents, and the sum of the minimum E-Value exponents are shown. To assist in thee comparison, these three metrics are shown ordered in Figure S10. It is clear from this Figure that Δ8THC exposure features close to the top of the list in Panel A, second top of the list in Panel B, and in first place (cumulative minimum E-Value exponents) in Panel C.

As it was of interest to consider the interactive effects of the tobacco:alcohol:Δ8THC interaction, an inverse probability weighted interactive model including this three-way interaction was also considered. A total of 202 significant positive terms are listed in Table S12. Importantly, the first 43 terms in this table all include Δ8THC. Remarkably, 36 minimum E-Values were listed as infinite and 80 were above 1000. Table 2 extracts from this list 49 terms including Δ8THC and notes that 36 mEVs were infinite and 48/49 (97.9%) mEVs were above 100,000,000. Thirty cancers were included on this list. Table 3 summarizes these results by covariate in tabular form and there are presented graphically in Figure 3. Once again, terms including Δ8THC appeared toward the right of these bar charts. In Panel C, terms incorporating Δ8THC occupied the top four positions on the graph for cumulative mEVs, with the leading position taken by the tobacco:Δ8THC interaction.

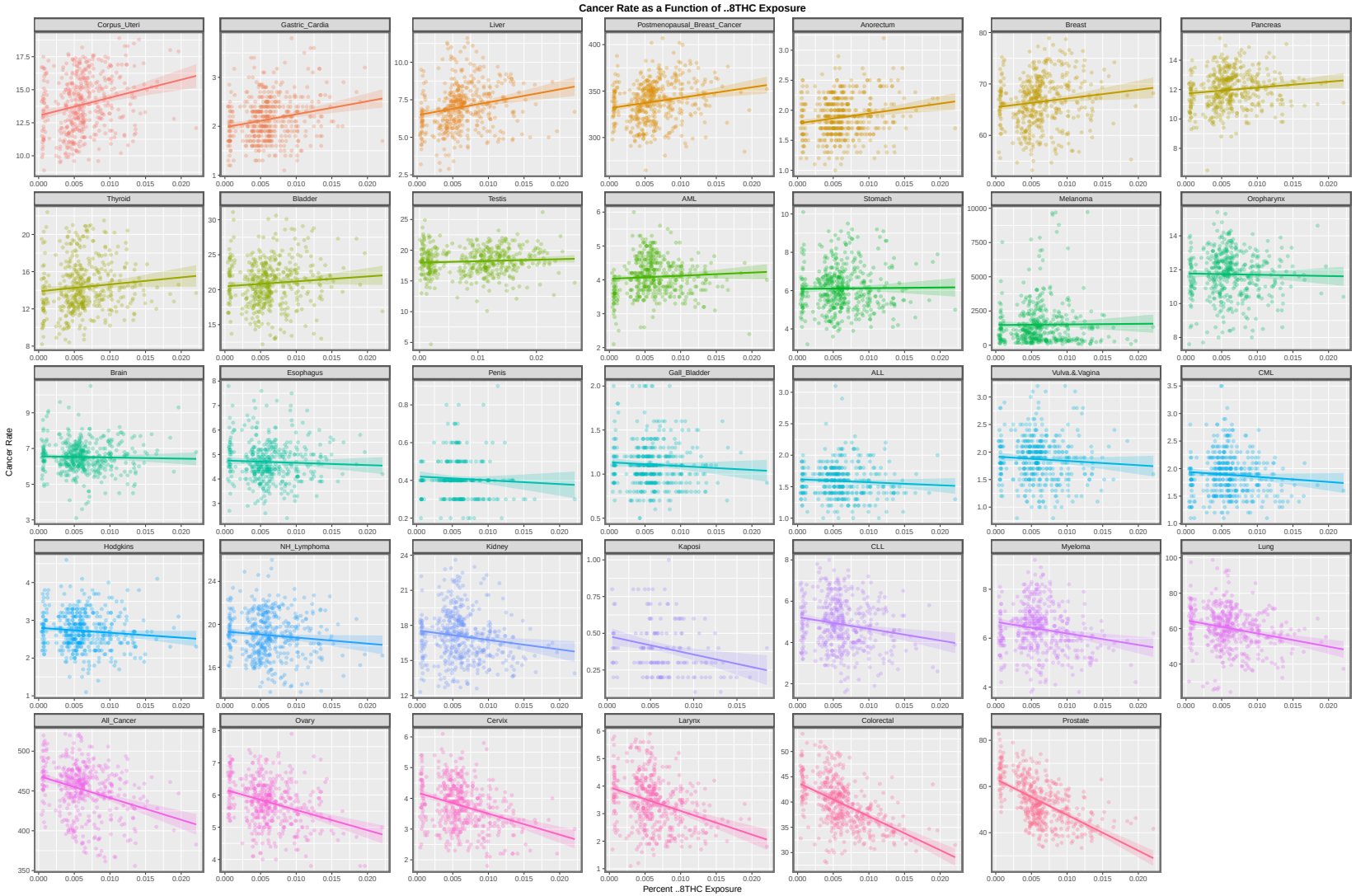


**Figure 2.** The bivariate continuous relationships of the Δ8THC rates by cancer type.

**Table 1.** The continuous bivariate relationships of Δ8THC.

| Cancer | Cases in Quintile 5 | Non-Cases in Quintile 5 | Cases in Quintile 1 | Non-Cases in Quintile 1 | R.R. | R.R. (Lower C.I.) | R.R. (Upper C.I.) | A.F.E. | A.F.E. (Lower C.I.) | A.F.E. (Upper C.I.) | P.A.R. | P.A.R. (Lower C.I.) | P.A.R. (Upper C.I.) | Chi. Squared | *p*-Value | E-Value Estimate | E-Value (Lower C.I.) |
|---|---|---|---|---|---|---|---|---|---|---|---|---|---|---|---|---|---|
| Melanoma | 100,207 | 384,314,333 | 115,471 | 540,452,122 | 1.2203 | 1.2100 | 1.2307 | 0.1805 | 0.1736 | 0.1874 | 0.0839 | 0.0803 | 0.0875 | 2134.601 | 0 | 1.74 | 1.71 |
| Liver | 49,147 | 384,365,393 | 62,900 | 540,504,693 | 1.0987 | 1.0859 | 1.1118 | 0.0899 | 0.0791 | 0.1005 | 0.0394 | 0.0344 | 0.0444 | 244.865 | $1.71 \times 10^{-55}$ | 1.43 | 1.39 |
| Corpus_Uteri | 78,333 | 384,336,207 | 100,741 | 540,466,852 | 1.0934 | 1.0833 | 1.1037 | 0.0854 | 0.0769 | 0.0939 | 0.0374 | 0.0334 | 0.0413 | 351.830 | $8.46 \times 10^{-79}$ | 1.41 | 1.38 |
| Anorectum | 10,462 | 384,404,078 | 13,537 | 540,554,056 | 1.0868 | 1.0594 | 1.1149 | 0.0799 | 0.0561 | 0.1030 | 0.0348 | 0.0240 | 0.0455 | 40.895 | $8.03 \times 10^{-11}$ | 1.39 | 1.31 |
| Thyroid | 67,875 | 384,346,665 | 89,788 | 540,477,805 | 1.0630 | 1.0525 | 1.0737 | 0.0593 | 0.0499 | 0.0686 | 0.0255 | 0.0213 | 0.0297 | 144.443 | $1.42 \times 10^{-33}$ | 1.32 | 1.29 |
| Gastric_Cardia | 144,970 | 384,269,570 | 193,373 | 540,374,220 | 1.0542 | 1.0471 | 1.0614 | 0.0514 | 0.0450 | 0.0579 | 0.0220 | 0.0192 | 0.0249 | 231.159 | $1.67 \times 10^{-52}$ | 1.29 | 1.27 |
| AML | 23,937 | 384,390,603 | 31,708 | 540,535,885 | 1.0616 | 1.0439 | 1.0795 | 0.0580 | 0.0421 | 0.0737 | 0.0250 | 0.0179 | 0.0320 | 48.720 | $1.48 \times 10^{-12}$ | 1.32 | 1.26 |
| Pancreas | 67,490 | 384,347,050 | 90,446 | 540,477,147 | 1.0493 | 1.0389 | 1.0598 | 0.0470 | 0.0374 | 0.0564 | 0.0201 | 0.0159 | 0.0242 | 89.545 | $1.50 \times 10^{-21}$ | 1.28 | 1.24 |
| Postmenopausal Breast Cancer | 249,834 | 384,164,706 | 337,900 | 540,229,693 | 1.0397 | 1.0344 | 1.0451 | 0.0382 | 0.0332 | 0.0432 | 0.0162 | 0.0141 | 0.0184 | 218.017 | $1.22 \times 10^{-49}$ | 1.24 | 1.22 |
| Breast | 337,544 | 384,076,996 | 462,078 | 540,105,515 | 1.0272 | 1.0227 | 1.0318 | 0.0265 | 0.0222 | 0.0308 | 0.0112 | 0.0093 | 0.0130 | 140.859 | $8.63 \times 10^{-33}$ | 1.19 | 1.17 |
| Testis | 52,627 | 1,726,611,593 | 19,713 | 670,166,199 | 1.0362 | 1.0194 | 1.0533 | 0.0349 | 0.0190 | 0.0506 | 0.0254 | 0.0137 | 0.0369 | 18.136 | $1.03 \times 10^{-5}$ | 1.23 | 1.16 |
| Oropharynx | 63,178 | 384,351,362 | 87,440 | 540,480,153 | 1.0160 | 1.0057 | 1.0265 | 0.0158 | 0.0057 | 0.0258 | 0.0066 | 0.0023 | 0.0109 | 9.276 | 0.0012 | 1.14 | 1.08 |
| Myeloma | 31,335 | 384,383,205 | 44,787 | 540,522,806 | 0.9838 | 0.9697 | 0.9982 | −0.0164 | −0.0312 | −0.0019 | −0.0068 | −0.0128 | −0.0008 | 4.889 | 0.0135 | 1.15 | - |
| Bladder | 103,627 | 384,310,913 | 148,415 | 540,419,178 | 0.9819 | 0.9741 | 0.9897 | −0.0185 | −0.0266 | −0.0104 | −0.0076 | −0.0109 | −0.0043 | 20.478 | $3.02 \times 10^{-6}$ | 1.16 | - |
| Vulva.&.Vagina | | 375,122,812 | 20,981 | 536,846,206 | 0.9803 | 0.9597 | 1.0013 | −0.0201 | −0.0420 | 0.0013 | −0.0082 | −0.0169 | 0.0005 | 3.370 | 0.0332 | 1.16 | - |
| CML | 9482 | 373,925,516 | 13,840 | 532,699,861 | 0.9760 | 0.9509 | 1.0019 | −0.0246 | −0.0517 | 0.0019 | −0.0100 | −0.0208 | 0.0007 | 3.313 | 0.0344 | 1.18 | - |
| Penis | 2283 | 312,646,824 | 3380 | 451,235,667 | 0.9749 | 0.9244 | 1.0280 | −0.0258 | −0.0817 | 0.0272 | −0.0104 | −0.0323 | 0.0110 | 0.884 | 0.1736 | 1.19 | - |
| Esophagus | 23,815 | 382,573,677 | 34,228 | 535,139,818 | 0.9732 | 0.9573 | 0.9895 | −0.0275 | −0.0446 | −0.0106 | −0.0113 | −0.0182 | −0.0044 | 10.330 | $6.54 \times 10^{-4}$ | 1.20 | - |
| ALL | 6865 | 344,103,689 | 9149 | 445,794,343 | 0.9721 | 0.9422 | 1.0030 | −0.0287 | −0.0614 | 0.0030 | −0.0123 | −0.0260 | 0.0012 | 3.140 | 0.0382 | 1.20 | - |
| Brain | 29,472 | 384,385,068 | 42,767 | 540,524,826 | 0.9691 | 0.9548 | 0.9835 | −0.0319 | −0.0474 | −0.0167 | −0.0130 | −0.0192 | −0.0069 | 17.236 | $1.65 \times 10^{-5}$ | 1.21 | - |
| Kidney | 82,655 | 384,331,885 | 120,241 | 540,447,352 | 0.9666 | 0.9581 | 0.9752 | −0.0345 | −0.0437 | −0.0254 | −0.0141 | −0.0177 | −0.0104 | 56.391 | $2.97 \times 10^{-14}$ | 1.22 | - |
| NH_Lymphoma | 93,104 | 384,321,436 | 137,276 | 540,430,317 | 0.9537 | 0.9458 | 0.9617 | −0.0485 | −0.0573 | −0.0398 | −0.0196 | −0.0230 | −0.0162 | 124.585 | $3.14 \times 10^{-29}$ | 1.27 | - |
| Gall_Bladder | 14,123 | 370,777,042 | 21,633 | 534,521,894 | 0.9412 | 0.9214 | 0.9613 | −0.0625 | −0.0853 | −0.0402 | −0.0247 | −0.0333 | −0.0161 | 31.433 | $1.03 \times 10^{-8}$ | 1.32 | - |
| Stomach | 32,140 | 384,382,400 | 48,205 | 540,519,388 | 0.9376 | 0.9244 | 0.9509 | −0.0666 | −0.0817 | −0.0516 | −0.0266 | −0.0324 | −0.0209 | 80.166 | $1.72 \times 10^{-19}$ | 1.33 | - |
| All_Cancer | 2,151,597 | 382,262,943 | 3,244,348 | 537,323,245 | 0.9326 | 0.9310 | 0.9342 | −0.0723 | −0.0741 | −0.0705 | −0.0288 | −0.0295 | −0.0281 | 6343.397 | 0 | 1.35 | - |
| Hodgkins | 10,210 | 384,404,330 | 15,405 | 540,552,188 | 0.9320 | 0.9090 | 0.9556 | −0.0730 | −0.1001 | −0.0465 | −0.0291 | −0.0394 | −0.0189 | 30.469 | $1.70 \times 10^{-8}$ | 1.35 | - |
| CLL | 26,057 | 384,388,483 | 39,705 | 540,527,888 | 0.9228 | 0.9085 | 0.9374 | −0.0836 | −0.1007 | −0.0668 | −0.0331 | −0.0395 | −0.0267 | 101.487 | $3.60 \times 10^{-24}$ | 1.38 | - |
| Ovary | 26,688 | 384,387,852 | 43,321 | 540,524,272 | 0.8663 | 0.8532 | 0.8796 | −0.1543 | −0.1721 | −0.1369 | −0.0588 | −0.0650 | −0.0527 | 340.797 | $2.14 \times 10^{-76}$ | 1.58 | - |
| Lung | 272,701 | 384,141,839 | 452,339 | 540,115,254 | 0.8478 | 0.8437 | 0.8518 | −0.1796 | −0.1852 | −0.1740 | −0.0675 | −0.0695 | −0.0656 | 4654.942 | 0 | 1.64 | - |
| Cervix | 14,961 | 384,399,579 | 25,037 | 540,542,556 | 0.8403 | 0.8234 | 0.8575 | −0.1901 | −0.2144 | −0.1662 | −0.0711 | −0.0792 | −0.0630 | 284.293 | $4.36 \times 10^{-64}$ | 1.67 | - |
| Colorectal | 171,103 | 384,243,437 | 286,861 | 540,280,732 | 0.8388 | 0.8338 | 0.8438 | −0.1922 | −0.1994 | −0.1851 | −0.0718 | −0.0742 | −0.0694 | 3323.813 | 0 | 1.67 | - |
| Larynx | 14,027 | 384,400,513 | 26,349 | 540,541,244 | 0.7486 | 0.7334 | 0.7641 | −0.3358 | −0.3635 | −0.3087 | −0.1167 | −0.1246 | −0.1087 | 772.855 | $2.15 \times 10^{-170}$ | 2.01 | - |
| Prostate | 218,368 | 384,196,172 | 413,423 | 540,154,170 | 0.7428 | 0.7389 | 0.7466 | −0.3463 | −0.3533 | −0.3394 | −0.1197 | −0.1217 | −0.1177 | 12739.787 | 0 | 2.03 | - |
| Kaposi | 1270 | 177,333,272 | 1589 | 143,565,460 | 0.6471 | 0.6010 | 0.6966 | −0.5455 | −0.6638 | −0.4356 | −0.2423 | −0.2837 | −0.2023 | 135.891 | $1.05 \times 10^{-31}$ | 2.46 | - |

**Table 2.** The positive significant terms including Δ8THC from the interactive panel model.

| Cancer | Term | Estimate | Std. Error | t-Statistic | S.D. | Adj. R. Squared | *p*-Value | E-Value Estimate | E-Value (Lower C.I.) |
|---|---|---|---|---|---|---|---|---|---|
| All_Cancer | cigmon: Δ8THC | 798.48 | 80.06 | 9.97 | 0.24 | 0.27 | $3.15 \times 10^{-21}$ | Infinity | Infinity |
| Lung | cigmon: Δ8THC | 2052.34 | 228.44 | 8.98 | 0.68 | 0.31 | $8.11 \times 10^{-18}$ | Infinity | Infinity |
| Stomach | cigmon: Δ8THC | 3221.86 | 395.94 | 8.14 | 1.17 | 0.02 | $4.33 \times 10^{-15}$ | Infinity | Infinity |
| Gall_Bladder | cigmon: Δ8THC | 2700.28 | 340.42 | 7.93 | 0.99 | −0.04 | $2.32 \times 10^{-14}$ | Infinity | Infinity |
| NH_Lymphoma | cigmon: Δ8THC | 1326.92 | 170.89 | 7.76 | 0.51 | 0.01 | $5.96 \times 10^{-14}$ | Infinity | Infinity |
| Kidney | cigmon: Δ8THC | 1253.70 | 162.80 | 7.70 | 0.48 | 0.09 | $9.27 \times 10^{-14}$ | Infinity | Infinity |
| CML | cigmon: Δ8THC | 2204.88 | 308.65 | 7.14 | 0.88 | 0.00 | $4.42 \times 10^{-12}$ | Infinity | Infinity |
| Thyroid | cigmon: Δ8THC | 1681.77 | 242.80 | 6.93 | 0.72 | −0.01 | $1.57 \times 10^{-11}$ | Infinity | Infinity |
| Vulva.&.Vagina | cigmon: Δ8THC | 2190.07 | 328.80 | 6.66 | 0.97 | 0.04 | $8.29 \times 10^{-11}$ | Infinity | Infinity |
| Bladder | cigmon: Δ8THC | 1224.02 | 190.07 | 6.44 | 0.56 | 0.22 | $3.18 \times 10^{-10}$ | Infinity | Infinity |
| Pancreas | cigmon: Δ8THC | 1553.31 | 245.48 | 6.33 | 0.73 | 0.06 | $6.22 \times 10^{-10}$ | Infinity | Infinity |
| Cervix | cigmon: Δ8THC | 1859.44 | 320.08 | 5.81 | 0.95 | 0.08 | $1.22 \times 10^{-8}$ | Infinity | Infinity |
| NH_Lymphoma | Δ8THC: AUD | 2282.42 | 393.82 | 5.80 | 0.51 | 0.01 | $1.31 \times 10^{-8}$ | Infinity | Infinity |
| Stomach | Δ8THC: AUD | 5230.42 | 912.47 | 5.73 | 1.17 | 0.02 | $1.86 \times 10^{-8}$ | Infinity | Infinity |
| Prostate | cigmon: Δ8THC: AUD | 8926.85 | 1562.45 | 5.71 | 0.39 | 0.26 | $2.06 \times 10^{-8}$ | Infinity | Infinity |
| All_Cancer | Δ8THC: AUD | 1052.81 | 184.49 | 5.71 | 0.24 | 0.27 | $2.14 \times 10^{-8}$ | Infinity | Infinity |
| Lung | Δ8THC: AUD | 2939.06 | 526.46 | 5.58 | 0.68 | 0.31 | $4.19 \times 10^{-8}$ | Infinity | Infinity |
| Corpus_Uteri | cigmon: Δ8THC | 1158.96 | 213.51 | 5.43 | 0.63 | 0.13 | $9.50 \times 10^{-8}$ | Infinity | Infinity |
| Melanoma | cigmon: Δ8THC: AUD | 56,176.95 | 10656.53 | 5.27 | 2.64 | 0.04 | $2.14 \times 10^{-7}$ | Infinity | Infinity |
| ALL | cigmon: Δ8THC: AUD | 34,385.14 | 6634.60 | 5.18 | 1.53 | −0.04 | $3.67 \times 10^{-7}$ | Infinity | Infinity |
| Colorectal | Δ8THC: AUD | 1353.86 | 266.99 | 5.07 | 0.34 | 0.15 | $5.88 \times 10^{-7}$ | Infinity | Infinity |
| CML | Δ8THC: AUD | 3523.42 | 702.47 | 5.02 | 0.88 | 0.00 | $8.01 \times 10^{-7}$ | Infinity | Infinity |
| Colorectal | cigmon: Δ8THC | 553.21 | 115.85 | 4.78 | 0.34 | 0.15 | $2.46 \times 10^{-6}$ | Infinity | Infinity |

**Table 3.** The summary of all terms from Δ8THC from the interactive panel model.

| Covariate | Number of Cancers | Total Negative Exponent of *p*-Value | Total Negative Exponent of Lower E-Value Bound |
|---|---|---|---|
| AIAN American | 14 | 48 | 10 |
| AUD | 15 | 73 | 171 |
| Cigarettes | 6 | 31 | 24 |
| Cigarettes: AUD | 8 | 19 | 208 |
| Cigarettes: Δ8THC | 19 | 183 | 4973 |
| Cigarettes: Δ8THC: AUD | 7 | 30 | 1884 |
| Δ8THC | 7 | 29 | 310 |
| AUD: Δ8THC | 16 | 73 | 4404 |
| Analgesics | 12 | 287 | 0 |
| Asian American | 21 | 121 | 0 |
| African_American | 21 | 428 | 0 |
| Cocaine | 11 | 68 | 0 |
| Hispanic_American | 5 | 11 | 0 |
| Median Income | 8 | 93 | 0 |
| NHPI_American | 10 | 70 | 53 |
| Caucasian American | 22 | 245 | 7 |

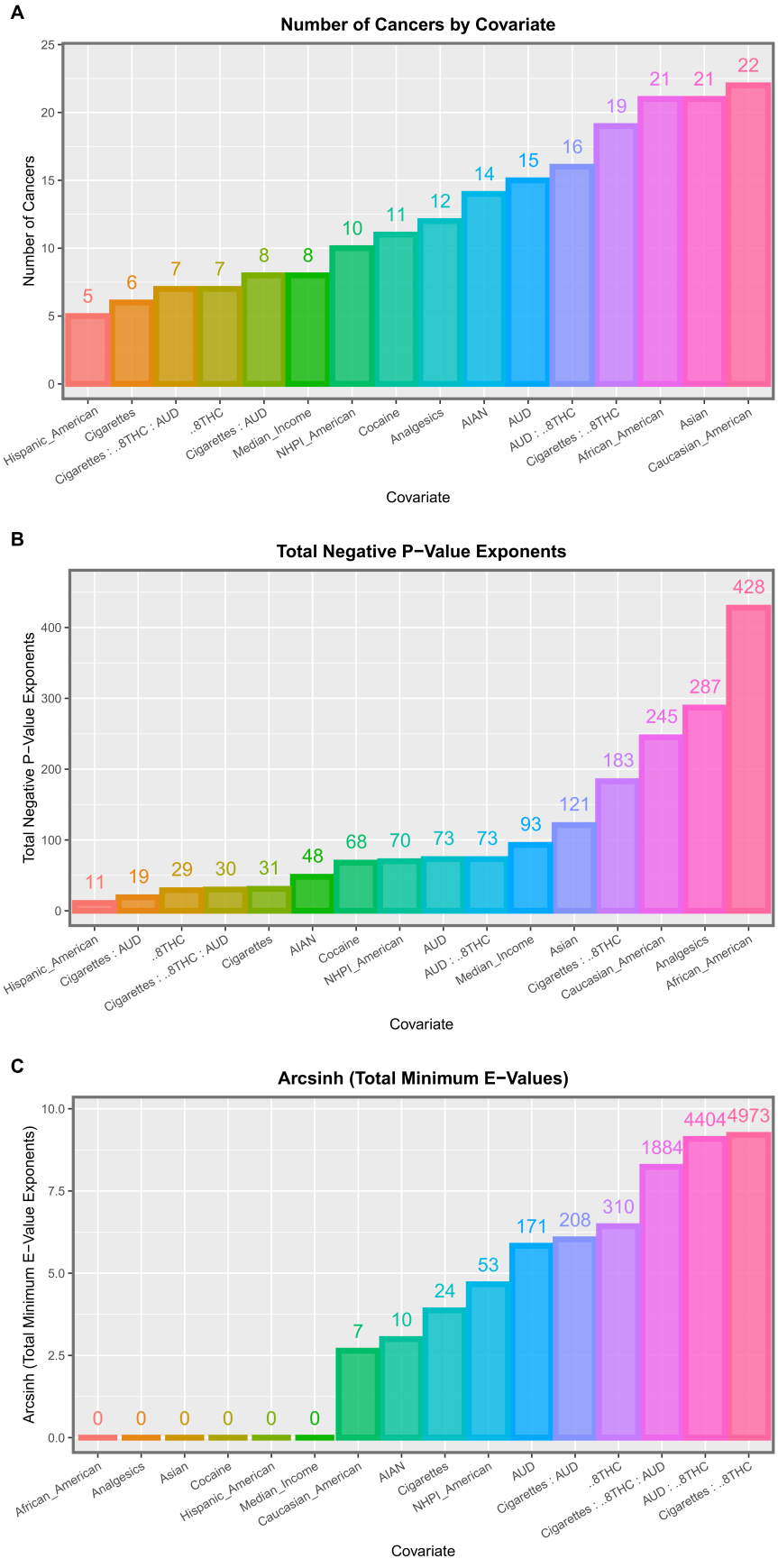


**Figure 3.** Summary graphs for the interactive multivariable panel models. Please see text for details.

### 3.4. Temporally Lagged Panel Models

#### 3.4.1. Two Years Temporal Lag

The same exercise may be conducted with all independent variables lagged by two years. An inverse probability weighted panel model including the same three-way tobacco:alcohol:Δ8THC interaction was therefore considered. A total of 179 positive and significant terms from such models are shown in Table S13. Again. 39 terms were noted to have infinite mEVs and Δ8THC was noted to be included in interactive terms in the first 40 positions. Table S14 extracts the terms including Δ8THC and it may be observed that 32 (78.0%) mEVs were infinite, and all exceeded $10^{12}$. Twenty-eight different tumor types were included on this list. These data are summarized by covariate in Table S15 and are presented graphically in Figure S11. In this figure, terms including Δ8THC were noted to occupy the mid-range of the number of tumors implicated and the significance levels, but the highest range for the cumulative mEVs (Panel C).

#### 3.4.2. Four Years Temporal Lag

As cancer is a disease that is believed to usually have a long incubation period, it is also of interest to consider models lagged to four years. For these purposes, the above interactive inverse probability (IPW) weighted model lagged to four years in all independent covariates was considered. Table S16 presents the 182 significant positive terms from this model. Table 4 extracts the 49 terms including Δ8THC, which relate to 25 tumor types. Remarkably, 48 terms (97.9%) had positive mEVs and the remaining one was $2.30 \times 10^{123}$. These data are summarized in tabular and graphical formats in Table S17 and Figure 4. In Panel A, terms including Δ8THC were found in the mid-position of the graph. In Panel B (cumulative significance levels), terms including Δ8THC occurred at the right end extreme of the graph. In panel C, which lists the cumulative mEVs, all four positions at the top of the graph were occupied by terms including Δ8THC.

#### 3.4.3. Marginal Effects

Given that the independent variables each have their own scale and in interactive models it can be difficult to tell what the overall or "marginal" effect of the covariates might be, it is of interest to consider the marginal effect of these covariates in additive, interactive, and lagged models. The marginal effect was calculated in units of the standard deviation of the dependent variable, the cancer rate. Table S18 shows the average marginal effect by tumor and substance type for the additive model. Fifteen cancer types were noted to have positive average marginal effects (AME). Tables S19–S21 undertook the same exercise for the interactive, two and four lag models and noted that 18, 17, and 10 cancers were associated with positive marginal effects. These findings are presented graphically in the heatmaps of Figure 5 and Figure S12–S14.

**Table 4.** Significant terms including Δ8THC from the interactive panel model at four years lag.

| Cancer | Term | Estimate | Std. Error | t-Statistic | S.D. | Adj. R. Squared | *p*-Value | E-Value Estimate | E-Value (Lower C.I.) |
|---|---|---|---|---|---|---|---|---|---|
| Kidney | lag(cigmon, 4): lag(Δ8THC, 4): lag(AUD, 4) | 20,775.83 | 729.67 | 28.47 | 0.35 | −0.03 | $8.04 \times 10^{-78}$ | Infinity | Infinity |
| AML | lag(Δ8THC, 4): lag(AUD, 4) | 37,051.70 | 1513.53 | 24.48 | 0.72 | −0.06 | $2.36 \times 10^{-66}$ | Infinity | Infinity |
| Pancreas | lag(Δ8THC, 4): lag(AUD, 4) | 30,354.71 | 1244.74 | 24.39 | 0.60 | −0.06 | $4.51 \times 10^{-66}$ | Infinity | Infinity |
| Kidney | lag(cigmon, 4): lag(Δ8THC, 4) | 6008.51 | 278.08 | 21.61 | 0.35 | −0.03 | $1.44 \times 10^{-57}$ | Infinity | Infinity |
| AML | lag(cigmon, 4): lag(Δ8THC, 4) | 11,523.47 | 576.82 | 19.98 | 0.72 | −0.06 | $2.09 \times 10^{-52}$ | Infinity | Infinity |
| Larynx | lag(Δ8THC, 4): lag(AUD, 4) | 42,033.01 | 2140.10 | 19.64 | 1.02 | 0.12 | $2.54 \times 10^{-51}$ | Infinity | Infinity |
| Brain | lag(cigmon, 4): lag(Δ8THC, 4): lag(AUD, 4) | 103,777.35 | 5628.18 | 18.44 | 0.63 | −0.06 | $2.01 \times 10^{-47}$ | Infinity | Infinity |
| Pancreas | lag(cigmon, 4): lag(Δ8THC, 4) | 8433.65 | 474.38 | 17.78 | 0.60 | −0.06 | $2.93 \times 10^{-45}$ | Infinity | Infinity |
| Vulva.&.Vagina | lag(cigmon, 4): lag(Δ8THC, 4) | 13,904.77 | 815.61 | 17.05 | 1.02 | 0.12 | $7.47 \times 10^{-43}$ | Infinity | Infinity |
| All_Cancer | lag(Δ8THC, 4): lag(AUD, 4) | 4404.42 | 263.84 | 16.69 | 0.13 | 0.11 | $1.12 \times 10^{-41}$ | Infinity | Infinity |
| Brain | lag(Δ8THC, 4) | 1766.26 | 115.19 | 15.33 | 0.63 | −0.06 | $3.70 \times 10^{-37}$ | Infinity | Infinity |
| Liver | lag(Δ8THC, 4): lag(AUD, 4) | 15,683.99 | 1078.13 | 14.55 | 0.52 | 0.22 | $1.52 \times 10^{-34}$ | Infinity | Infinity |
| ALL | lag(cigmon, 4): lag(Δ8THC, 4): lag(AUD, 4) | 80,386.15 | 6115.36 | 13.14 | 0.66 | −0.08 | $3.84 \times 10^{-28}$ | Infinity | Infinity |
| Liver | lag(cigmon, 4): lag(Δ8THC, 4) | 4887.56 | 410.89 | 11.90 | 0.52 | 0.22 | $8.25 \times 10^{-26}$ | Infinity | Infinity |
| ALL | lag(Δ8THC, 4) | 1491.45 | 125.55 | 11.88 | 0.66 | −0.08 | $1.96 \times 10^{-24}$ | Infinity | Infinity |
| Oropharynx | lag(cigmon, 4): lag(Δ8THC, 4): lag(AUD, 4) | 42,596.04 | 3835.11 | 11.11 | 0.43 | 0.27 | $2.79 \times 10^{-23}$ | Infinity | Infinity |
| EsophLagus | lag(cigmon, 4): lag(Δ8THC, 4): lag(AUD, 4) | 79,727.71 | 7246.10 | 11.00 | 0.80 | −0.06 | $8.94 \times 10^{-23}$ | Infinity | Infinity |
| All_Cancer | lag(cigmon, 4): lag(Δ8THC, 4) | 1092.50 | 100.55 | 10.87 | 0.13 | 0.11 | $1.63 \times 10^{-22}$ | Infinity | Infinity |
| CLL | lag(Δ8THC, 4): lag(AUD, 4) | 16,144.24 | 1490.78 | 10.83 | 0.71 | 0.09 | $2.11 \times 10^{-22}$ | Infinity | Infinity |
| NH_Lymphoma | lag(Δ8THC, 4): lag(AUD, 4) | 11,559.70 | 1096.50 | 10.54 | 0.52 | −0.03 | $1.68 \times 10^{-21}$ | Infinity | Infinity |

**Table 4.** *Cont.*

| Cancer | Term | Estimate | Std. Error | t-Statistic | S.D. | Adj. R. Squared | *p*-Value | E-Value Estimate | E-Value (Lower C.I.) |
|---|---|---|---|---|---|---|---|---|---|
| EsophLagus | lag(Δ8THC, 4) | 1551.04 | 148.10 | 10.47 | 0.80 | −0.06 | $3.93 \times 10^{-21}$ | Infinity | Infinity |
| Oropharynx | lag(Δ8THC, 4) | 765.23 | 78.49 | 9.75 | 0.43 | 0.27 | $4.72 \times 10^{-19}$ | Infinity | Infinity |
| Myeloma | lag(cigmon, 4): lag(Δ8THC, 4): lag(AUD, 4) | 51,756.76 | 5401.86 | 9.58 | 0.61 | 0.02 | $1.52 \times 10^{-18}$ | Infinity | Infinity |
| Postmenopausal Breast Cancer | lag(cigmon, 4): lag(Δ8THC, 4): lag(AUD, 4) | 23,566.70 | 2616.35 | 9.01 | 0.29 | 0.10 | $7.76 \times 10^{-17}$ | Infinity | Infinity |
| Postmenopausal Breast Cancer | lag(Δ8THC, 4) | 461.33 | 53.55 | 8.61 | 0.29 | 0.10 | $1.07 \times 10^{-15}$ | Infinity | Infinity |
| Bladder | lag(Δ8THC, 4): lag(AUD, 4) | 11,273.58 | 1317.42 | 8.56 | 0.63 | 0.06 | $1.57 \times 10^{-15}$ | Infinity | Infinity |
| Anorectum | lag(Δ8THC, 4): lag(AUD, 4) | 16,569.38 | 1977.38 | 8.38 | 0.95 | −0.02 | $5.04 \times 10^{-15}$ | Infinity | Infinity |
| CLL | lag(cigmon, 4): lag(Δ8THC, 4) | 4683.01 | 568.15 | 8.24 | 0.71 | 0.09 | $1.23 \times 10^{-14}$ | Infinity | Infinity |
| Lung | lag(Δ8THC, 4): lag(AUD, 4) | 9636.37 | 1178.24 | 8.18 | 0.56 | 0.10 | $1.85 \times 10^{-14}$ | Infinity | Infinity |
| Myeloma | lag(Δ8THC, 4) | 856.96 | 110.56 | 7.75 | 0.61 | 0.02 | $2.81 \times 10^{-13}$ | Infinity | Infinity |
| Thyroid | lag(Δ8THC, 4): lag(AUD, 4) | 6736.53 | 885.15 | 7.61 | 0.42 | 0.18 | $6.73 \times 10^{-13}$ | Infinity | Infinity |
| Bladder | lag(cigmon, 4): lag(Δ8THC, 4) | 3651.37 | 502.08 | 7.27 | 0.63 | 0.06 | $5.33 \times 10^{-12}$ | Infinity | Infinity |
| Anorectum | lag(cigmon, 4): lag(Δ8THC, 4) | 4954.17 | 753.59 | 6.57 | 0.95 | −0.02 | $3.18 \times 10^{-}10$ | Infinity | Infinity |
| Prostate | lag(cigmon, 4): lag(Δ8THC, 4): lag(AUD, 4) | 16,430.44 | 2513.72 | 6.54 | 0.28 | 0.15 | $3.94 \times 10^{-}10$ | Infinity | Infinity |
| NH_Lymphoma | lag(cigmon, 4): lag(Δ8THC, 4) | 2661.93 | 417.88 | 6.37 | 0.52 | −0.03 | $9.98 \times 10^{-}10$ | Infinity | Infinity |
| Ovary | lag(cigmon, 4): lag(Δ8THC, 4): lag(AUD, 4) | 41,343.79 | 6533.78 | 6.33 | 0.73 | −0.02 | $1.26 \times 10^{-9}$ | Infinity | Infinity |
| Ovary | lag(Δ8THC, 4) | 806.38 | 133.73 | 6.03 | 0.73 | −0.02 | $6.38 \times 10^{-9}$ | Infinity | Infinity |
| Thyroid | lag(cigmon, 4): lag(Δ8THC, 4) | 1993.67 | 337.34 | 5.91 | 0.42 | 0.18 | $1.21 \times 10^{-8}$ | Infinity | Infinity |
| Breast | lag(cigmon, 4): lag(Δ8THC, 4): lag(AUD, 4) | 10,735.82 | 1828.95 | 5.87 | 0.21 | 0.30 | $1.49 \times 10^{-8}$ | Infinity | Infinity |
| Prostate | lag(Δ8THC, 4) | 299.18 | 51.45 | 5.82 | 0.28 | 0.15 | $1.99 \times 10^{-8}$ | Infinity | Infinity |

**Table 4.** *Cont.*

| Cancer | Term | Estimate | Std. Error | t-Statistic | S.D. | Adj. R. Squared | *p*-Value | E-Value Estimate | E-Value (Lower C.I.) |
|---|---|---|---|---|---|---|---|---|---|
| Breast | lag(Δ8THC, 4) | 210.27 | 37.43 | 5.62 | 0.21 | 0.30 | $5.51 \times 10^{-8}$ | Infinity | Infinity |
| Hodgkins | lag(Δ8THC, 4) | 1216.18 | 217.41 | 5.59 | 1.19 | 0.03 | $6.20 \times 10^{-8}$ | Infinity | Infinity |
| Lung | lag(cigmon, 4): lag(Δ8THC, 4) | 2417.46 | 449.04 | 5.38 | 0.56 | 0.10 | $1.78 \times 10^{-7}$ | Infinity | Infinity |
| Hodgkins | lag(cigmon, 4): lag(Δ8THC, 4): lag(AUD, 4) | 55,559.09 | 10,622.37 | 5.23 | 1.19 | 0.03 | $3.76 \times 10^{-7}$ | Infinity | Infinity |
| Vulva.&.Vagina | lag(cigmon, 4): lag(Δ8THC, 4): lag(AUD, 4) | 61,495.75 | 13,454.10 | 4.57 | 1.51 | −0.01 | $8.25 \times 10^{-6}$ | Infinity | Infinity |
| Stomach | lag(cigmon, 4): lag(Δ8THC, 4): lag(AUD, 4) | 33,237.10 | 7879.98 | 4.22 | 0.89 | −0.03 | $3.53 \times 10^{-5}$ | Infinity | Infinity |
| Stomach | lag(Δ8THC, 4) | 669.75 | 161.28 | 4.15 | 0.89 | −0.03 | $4.61 \times 10^{-5}$ | Infinity | Infinity |
| Corpus_Uteri | Caucasian American | 2187.58 | 1013.65 | 2.16 | 0.48 | −0.01 | $3.19 \times 10^{-2}$ | Infinity | Infinity |
| Vulva.&.Vagina | lag(Δ8THC, 4) | 1006.92 | 275.18 | 3.66 | 1.51 | −0.01 | $3.19 \times 10^{-4}$ | Infinity | $2.31 \times 10^{123}$ |

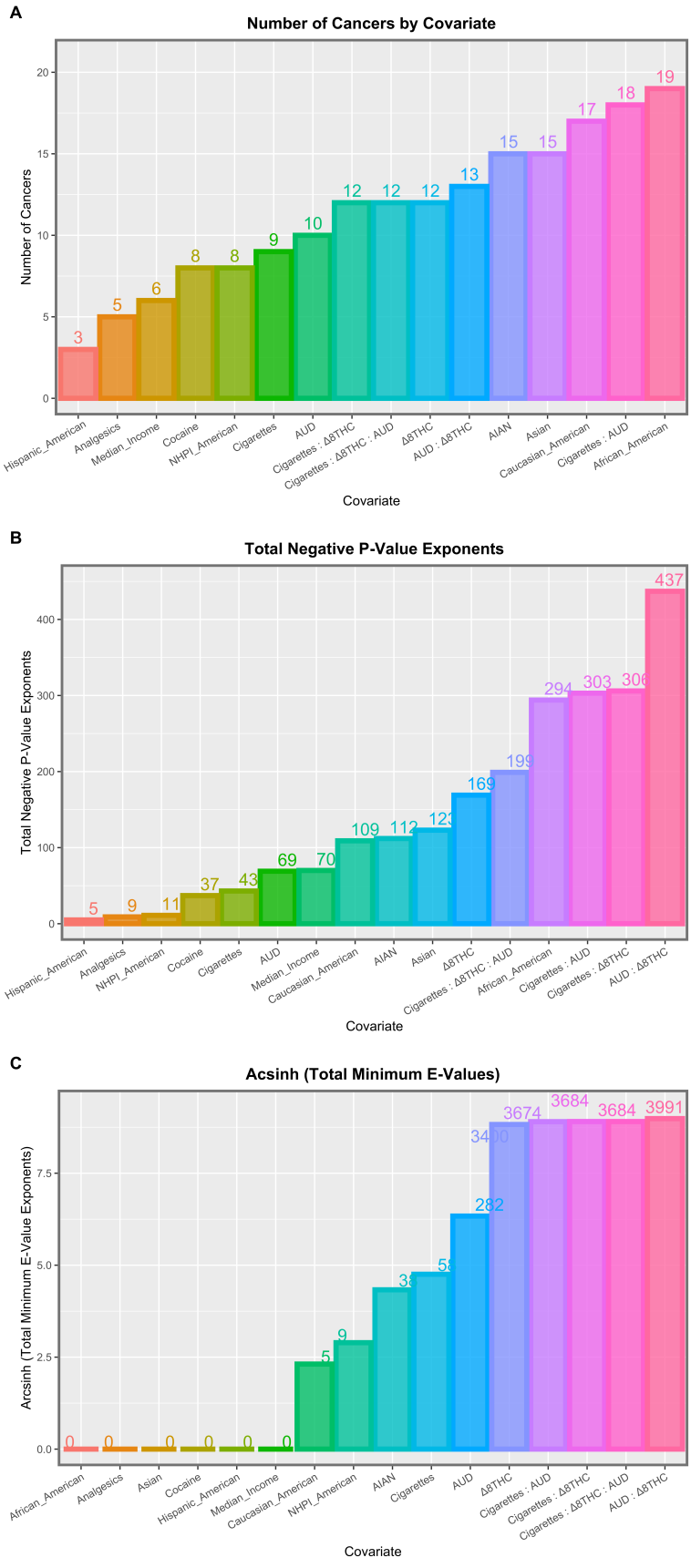


**Figure 4.** Summary graphs for the interactive multivariable panel models at four years of lag.

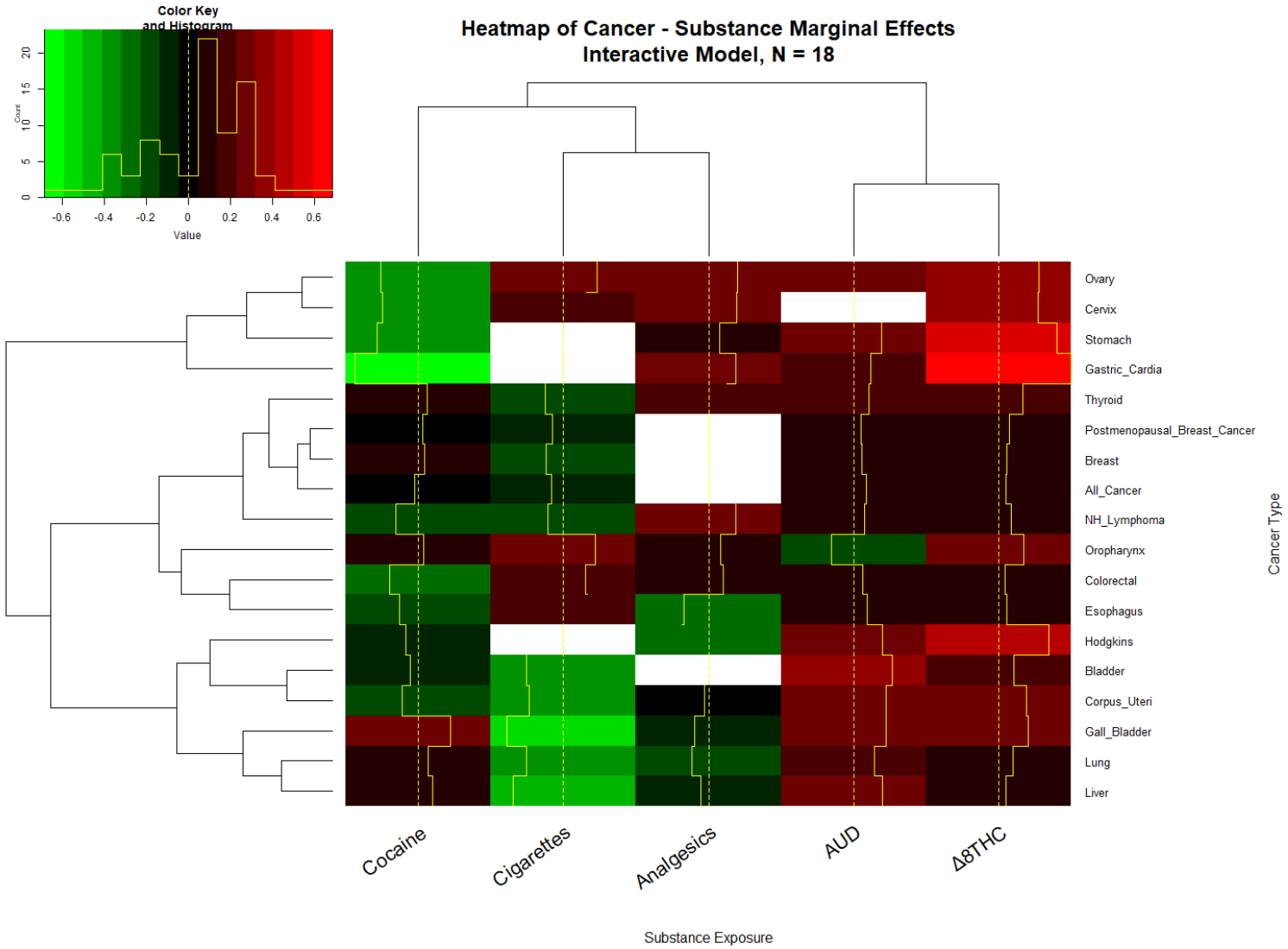


**Figure 5.** The heatmap of the cancer–substance marginal effects, Interactive IPW model.

Table 5 collates the AME data for the substances, shows the mean and standard deviation of the various tumor incidences, and calculates the change in the case numbers for each tumor. The totals are noted near the foot of the table. The applicable figures for "All cancers" are also provided. It is noted that the numbers for breast cancer exceeded that for all cancers as the incidence of that tumor type was calculated on a single sex. This table shows that the total number of cancers attributable to Δ8THC was an extra 8.58/100,000 compared to 7.93 for AUD and −8.48 for tobacco (for this group of cancers).

**Table 5.** A summary of all terms from Δ8THC from the interactive panel model at four years lag.

| Covariate | Number of Cancers | Total Negative Exponent of *p*-Value | Total Negative Exponent of Lower E-Value Bound |
|---|---|---|---|
| AIAN American | 15 | 112 | 38 |
| AUD | 10 | 69 | 282 |
| Cigarettes | 9 | 43 | 58 |
| Cigarettes: AUD | 18 | 303 | 3674 |
| Cigarettes: Δ8THC | 12 | 306 | 3684 |
| Cigarettes: Δ8THC: AUD | 12 | 199 | 3684 |
| Δ8THC | 12 | 169 | 3400 |
| AUD: Δ8THC | 13 | 437 | 3991 |
| Analgesics | 5 | 9 | 0 |
| Asian American | 15 | 123 | 0 |
| African_American | 19 | 294 | 0 |
| Cocaine | 8 | 37 | 0 |
| Hispanic_American | 3 | 5 | 0 |
| Median Income | 6 | 70 | 0 |
| NHPI_American | 8 | 11 | 9 |
| Caucasian American | 17 | 109 | 5 |

## 4. Discussion

### 4.1. Main Results

The study findings are remarkable as both the number of tumors to which the population Δ8THC exposure was related as well as the extraordinarily elevated degree of association demonstrated by the very high mEVs. In a straight bivariate continuous analysis, Δ8THC was shown to be significantly associated with eight cancers (corpus uteri, liver, gastric cardia, post-menopausal breast cancer, anorectum, pancreas, breast, and thyroid, Table S5) and a comparison of the highest and lowest quintiles of exposure showed that 12 cancers were significantly related to Δ8THC exposure on categorical analysis (additionally: melanoma, corpus uteri, anorectum, acute myeloid leukemia, pancreas, breast, testicular, and oropharynx, Table 1). In an additive IPW panel model adjusting for all substances, ethnicity, and median household income, 15 cancers were related to population Δ8THC exposure including stomach, Hodgkins, acute lymphoid leukemia, brain, breast, cervix, colorectal, and myeloma in addition to those above-mentioned (Table S10). An interactive panel model found significant positive terms for 30 cancer types which, in addition to those listed above included all cancers (excluding non-melanoma skin cancers), lung, gall bladder, Non-Hodgkins lymphoma, kidney, chronic myeloid and lymphoid leukemias, vulva and vaginal, esophagus, and prostate cancers.

Consideration of the category "All cancers" (excluding non-melanoma skin cancers) featured at the top of the terms for the interactive models ($p = 3.15 \times 10^{-21}$, mEV = infinity, Table 2), in the model lagged by two years ($p = 3.40 \times 10^{-3}$, mEV = infinity, Table S14),

and also at four lags ($p = 1.11 \times 10^{-41}$, mEV = infinity, Table 4). In a marginal effects study, Δ8THC was noted to have an effect equal to that of AUD and above that of tobacco. Additionally of note was the very high strength of the association of these tumors with Δ8THC, as quantified by the 95% lower bound of the E-Value. In the continuous analysis, elevated mEVs ranged from $3.42 \times 10^{15}$ to 27.14 (Table S5) and in the additive panel model, from $2.64 \times 10^{14}$ to 42.69 (Table S10). In the interactive IPW panel models lagged to zero, two, and four years, 73.5%, 80.5%, and 97.9% of 49, 41, and 49 elevated E-Values were infinite with mEVs declining from infinity in each case to 56.10, $2.85 \times 10^{12}$, and $2.31 \times 10^{123}$, respectively.

### 4.2. Mechanisms

A discussion of the mechanisms of Δ8THC's cellular actions is highly pertinent to the Hill criteria of causality under the biological plausibility clause [68]. Δ8THC is less well-studied in this respect than Δ9THC. Cells carry all the machinery of cannabinoid signal reception and transduction in the inner and outer membranes of mitochondria [17,20,21], which are in free and ready communication with the nucleus, and Δ8THC binds CB1R [2,5] and inhibits mitochondrial activity [17–21]. Mitochondria supply both small molecular epigenetic substrates and energy required for genome maintenance and stability and the epigenetic machinery. As was noted above, Δ8THC is known to inhibit DNA, RNA, and protein synthesis [5,6,36–39]. Extensions of such studies with Δ9THC showed that Δ9THC inhibited histone synthesis (in excess of 50%) [69,70], which necessarily leads to an open chromatin conformation and therefore has major effects on the availability of chromatin for transcription in a pro-oncogenic manner. Δ9THC has been shown to greatly alter DNA methylation in the sperm of mice, rats, and men [14–16,71,72], inducing changes that persist in altered brain and appetitive center function in subsequent generations [16,73,74], perturbations that have been shown to improve with cannabis abstinence [75]. Indeed, if one adds the length of the chromosomes (13,18, 21, X), recently shown to be affected by cannabis-induced trisomies/monosomy [27] to those affected in testicular carcinoma (1, 7, 8, 11, 12, 13, 18, 21, X, Y) [76] and commonly in acute lymphoid leukemia (4, 9, 10, 11, 22) [77], one arrives at the sizeable length of 1765 MB or 58.8% of the 3000 MB of the human genome directly impacted by chromosomal toxicity alone.

### 4.3. Mechanisms of Cannabinoid Carcinogenesis

The link between cancer and cannabinoids is complex and multifactorial and has recently been reviewed in several recently published works [10,14–16,27,31,32,34,35,41–43,71,72,75,78–92]. Our intention here is to introduce the way in which these general observations may relate to some specific cancer types. We also considered recent important epigenomic findings and mechanisms underlying chromosomal mis-segregation events and chromosomal breakage and translocation events that are known to be important oncogenic events underlying tumors such as acute myeloid and lymphoid leukemias and testicular cancer [25,76,77,93–95].

### 4.4. Recent DNA Methylation Studies

Of particular importance is the recent finding emerging from an epigenome wide association study (EWAS) of twenty cannabis dependent patients and twenty control subjects compared to each other both before and after an eleven week period of documented cannabis sobriety [75]. This study identified 810 hits relating to cancer-related terms (including "neoplasm", "carcinogenesis", "tumor", "carcinoma", "leukemia" and "lymphoma") and mentioned specifically cancers of the haemopoietic system (leukemia, lymphoma, myeloma), breast, ovarian, colorectal, prostate, brain, pancreatic, thyroid, liver, melanoma, esophageal, and gastric and upper respiratory tract tumors. Indeed, the cancer signal was one of the strongest overall signals to emerge from this EWAS. The full implications of this profound and far-reaching result have yet to be fully explored. They have an obvious

relevance and concordance with the results reported both in this study and in similar reports [27,79–81,96–98].

### 4.5. Chromosomal Structural Observations

#### 4.5.1. Shedding of Chromosomal Arms and Possible Breakage–Fusion–Bridge Cycles

Several classical studies have provided clear evidence of chromosomal breaks [9,10,13], end-to-end fusions [9,10], and chromosomal bridge formations in telophase [11,12,99] following cannabis exposure. Such findings suggest that the breakage–fusion–bridge cycle described by Barbara McClintock may be in operation [100,101] for all of the elements of this cycle have clearly been shown to be present. If such a positive feed-forward cycle were operating, it would explain the aggressive loss of 50–70 chromosomal arms from testicular tumor germ cells in the non-seminomatous germ cell tumors, which is well-established to be linked with cannabis [76]. It may be that careful experimental investigation of the mechanistic basis of this florid loss of chromosomal segments would be very informative.

#### 4.5.2. Errors of Meiosis and Mitosis

Hyperploidy and supernumerary chromosomal replication has been demonstrated following cannabis exposure in mammalian lymphocytes and oocytes [12,99]. Such a finding would be consistent with the one or two rounds of genomic doubling required in the biogenesis of testicular carcinogenesis [76].

Trisomies (of chromosomes 13, 18 and 21) and monosomies (of chromosome X, Turners syndrome) have been well-documented following cannabis exposure [44,46,47,81,102], where chromosomal mis-segregation is clearly a major feature of cannabis-related genotoxicity. Moreover, male disomy of chromosome X (Kleinfelters syndrome) has also been observed in association with cannabis exposure in the European data (manuscript submitted). Such strong epidemiological evidence of chromosomal mis-segregation is supported by the induction of lagging chromosomes following cannabis exposure [7,8,10,86,88,103] and by the well-known positive results of cannabis on testing in the micronucleus assay [104].

The mitotic spindle is comprised of microtubules that are polymers of tubulin [105]. Cannabis has been shown to inhibit tubulin synthesis [70]. Therefore, interference with the integrity of the mitotic spindle is one mechanism by which cannabinoids may disrupt cell division [105,106].

#### 4.5.3. Epigenomic Control of Chromosomal Centromeric Function

The binding of chromosomes to the mitotic spindle in mammals is mediated by the kinetochore, which is a large 90-protein complex that binds centromeric chromatin of each chromosome to 25–30 microtubules of the mitotic spindle [107]. Most of the arms of the mitotic spindle are actually incomplete and the spindle therefore is actually two half-spindles that are linked by complete rays, which course from one controller to the other. Chromosomes are bound to the growing plus ends of the half spindle rays. The chromosomes separate at anaphase due to the pulling forces exerted by dynein–dynactin molecular motors, which retract the chromosomes toward the minus ends of the microtubules and the new pronuclear poles [108–113].

The histones occurring in centromeric chromatin are specialized and mark this section of the chromatin uniquely. A group of CENP-A variants of histone 3 are some of the most important of these modified histones [114]. H3-CENP-As have been widely conserved across plant and animal phyla [115]. Pericentromeric histones are richly decorated in post-translational epigenomic modifications (PTM). SUMOylation is the addition of Small Ubiquitin-like MOdifier (SUMO) proteins and is one of the most important post-translational modifications, which becomes a key step in the formation of the rich and complex chains of PTMs including (methylation, acetylation, tyrosinylation, sulfation, phosphorylation, ubiquitylation, etc.), which then control kinetochore function combinatorially [116]. Specific PTMs that are controlled by sumoylation include H3K4me1, H3K4me2,

H3K4me3, H3- and H4-acetylation, and H2BK123 ubiquitination [116]. Thus, histone sumoylation acts as a key functional switch that controls the kinetochore function and its downstream signaling to release the Spindle Associated Checkpoint (SAC), which controls the anaphase segregation of chromosomes [107].

Therefore, the observation that this histone sumoylation switch is powerfully controlled by Δ9THC is of great relevance to the issue of chromosomal mis-segregation during anaphase and cytokinesis subsequent to cannabis exposure [117]. Ubiquitin-like-specific protease 2 (ulp2) is inhibited by Δ9THC, which blocks desumoylation and thereby disrupts the integrity of the sumoylation code [116]. Administration of Δ9THC to dividing cells thus causes major disruptions of the kinetochore signaling to the SAC and leads to errors of chromosomal segregation [116]. Δ9THC also directly affects murine double minute 2 (mdm2) and SUMO-1 protein major binding partners of P53, which is well-known as the classical "guardian of the genome" [117]. Through interference with mdm2 and SUMO-1, Δ9THC activates P53 directly. P53 in cannabis-exposed cells will thus be activated both canonically via the induction of DNA single- and double-stranded breaks and also via its protein interactome.

Thus, pericentromeric chromatin is regulated by a series of sophisticated epigenomic mechanisms through the critical stages of attachment to the mitotic spindle and chromosomal segregation, and cannabinoids seriously disrupt this complex post-translational interacting signalome. Since this centromeric epigenomic nucleosomal mechanism controls chromosomal segregation and may also be involved in chromosomal counting and identification systems, it becomes apparent that the disturbance of kinetochore function plays a pivotal and central role in both the induction of chromosomal mis-segregation errors, and likely hyperploidy and their downstream sequelae.

#### 4.5.4. Epigenomic Impacts on DNA Breakage Sites

Both single- and double- stranded breaks (SSB and DSB) are a common feature of cell karyotype studies after cannabis exposure [7–10,12,13,99]. It therefore becomes important in the present context to note that the epigenome plays an often determinative role in influencing or selecting the site of DNA breakage generally [118–131], during meiotic crossing over [132–139], in the immune gene hypervariable region [140–146], and in oncogenic pathways [120,123,124,147–154].

The presence of acute lymphoid leukemia (ALL) listed in Tables 2 and 4 in the present study is significant. This disorder is known to commonly represent end-to-end translocations and fusions between several chromosomes (such as 4 and 11, 9 and 22, 4 and 10) [77]. As well as in the present results, ALL was also recently shown to be elevated in association with population-wide cannabis exposure. The chromosomal and genomic lesions of this tumor imply increased chromosomal double-stranded breaks, and anomalous repair, resulting in the chromosomal translocation landscape described [77].

#### 4.5.5. Cannabinoids Deliver Multiple Carcinogenic Insults

The multi-hit hypothesis is one of the common models of carcinogenesis and involves multiple genotoxic or epigenotoxic hits to the genome, which result in genomic instability [94,155–158]. As cannabinoids can deliver both double- and single-stranded DNA breaks and cause the disruption of key kinetochore functions (hypoploidy [11], hyperploidy [12,99], and chromosomal mis-segregation [27,44,47,102]), it is clear that significant cannabinoid exposure can deliver multi-point genomic hits in themselves. This also explains the dramatic abnormalities of cell karyotype from the minimal cannabis exposure (just a few puffs) observed in many classical cell morphology studies [7–9,11,12,86,88,99].

Testicular carcinoma was noted to be elevated in Table 1. This tumor almost invariably involves the development of an isochromosome 12p. Its presence is explained by the concept of presumptive pericentromeric chromatin dysregulation as the dysregulated pericentromeric epigenome presumably facilitates the aberrant scission of the chromosome at the centromere, forming the isochromosome through the interactions between the

epigenome and the genome as described above [118–131]. The presence of KIT and KRAS (and to a lesser extent NRAS) on chromosome 12 then confers a growth advantage on the mutant clone, and malignant tumorigenesis is the end result of this process continued in the context of the gross re-sculpting of the chromosomal landscape by repeated cycles of the breakage–fusion–bridge cycle across multiple cell divisions that accumulate over time.

### *4.6. Causal Inference*

Qualitative Causal Inference. The qualitative criteria required of causal relationships were set out by Hill in 1965 [68] and it is noted that this study fulfills all these criteria, except those that require replication elsewhere, which is unavoidable in an initial study. Hence, the present results demonstrate the strength of association, specificity, temporality, coherence with known data, biological plausibility, a biological dose–response gradient, and experimental confirmation. In light of its pioneering nature, we were not able to demonstrate consistency amongst studies or analogy with similar situations elsewhere.

Quantitative Causal Inference. The use of inverse probability weighting in all panel models has the effects of making all groups in an observational study pseudo-randomized and allows for causal inferences to be drawn from observational data. Its results have recently been checked against later randomized control trials and these effects have been confirmed. Similarly E-Values, or the expected values, quantitates the degree of co-association required of some hypothetical external confounder variable with both the exposure and the outcome in order to explain away the observed effect. In the present study, the many very elevated mEVs at infinity preclude external explanations on the quantitative criteria, which is commonly used to indicate causal pathways above 1.25 [64]. As this study combined both inverse probability weighting and mEVs, it becomes a powerful framework within which to consider causal relationships.

### *4.7. Generalizability*

We feel that these results are generalizable for the quantitative reasons noted above because they fulfill the quantitative criteria of causal inference. Not only do these results fulfill the quantitative criteria, but they also fulfill most of the quantitative criteria of Hill [68] including the strength of association, specificity, temporality, coherence with other known data, biological plausibility, biological dose-response gradient, and experimental confirmation. As this is the first study of this type to our knowledge, the only criteria that is not met is that results have not been replicated elsewhere as this is the first study of this type to our knowledge. As the relationship appears to be defined causally, the expectation is that this link would be shown wherever data of sufficient quality exists.

### *4.8. Strengths and Limitations*

This study has a number of strengths and limitations. Its strengths include that it uses large national datasets with high response rates, that the analytical plan is relatively simple (continuous and categorical bivariate and multivariate) but also powerful including multiple simultaneous model processing (via purrr) and liberal use of the tools of causal inference, particularly inverse probability weighting and E-Values. Its limitations are that we had to rely on estimates of the state Δ8THC exposure as the actual data are not available, however, this is a common practice in such studies of the cancer epidemiology of individual cannabinoids [27,28,159]. Like many epidemiological studies, individual participant level data were not available to the present investigators. Whilst cancer-specific risk factors were not studied (such as hormonal exposure, body mass index, and regular exercise), the very high E-Values reported in this study (see Tables 2 and 4) indicate that the inclusion of such covariates would not greatly perturb the main results reported herein.

## 5. Conclusions

In conclusion, this study demonstrated that Δ8THC exposure may be directly linked to eight cancer types in bivariate testing and as many as 18 of the 34 tumor types assessed

on inverse panel regression persisted after full multivariable adjustment. The effect sizes reported herein were remarkably strong, often ranging up to infinity for the minimum E-Values of significant terms in multivariable models. The overall marginal effect shown was around 8.6/100,000, a figure comparable to alcohol and above that for tobacco. These results are consistent both with other recent reports of cannabinoid-related carcinogenesis in adults and children and a basic science genotoxic and epigenotoxic literature, which has long documented the genotoxicity and epigenotoxicity of multiple cannabinoids. Documented relationships fulfill both quantitative and qualitative criteria for causality. These results sound a strong note of warning that the present commercially driven renewed interest and popularity of Δ8THC in the USA may portend a major epidemic in years and generations to come of genotoxic including cancerogenic and other outcomes not only in the deliberately exposed, but also potentially spilling over into the food chain with effects on general communities, systemic and inheritable epigenomic aging, and having downstream outcomes for several generations to come.

**Supplementary Materials:** The following supporting information can be downloaded at: https://www.mdpi.com/article/10.3390/ijerph19137726/s1. Figure S1. Temporal trends in selected cannabinoid concentrations in USA FDA seizures, Figure S2. Map-graph of estimates of Δ8THC concentrations across USA over time. (Estimates derived as described in Methods section), Figure S3. Pannelled scatterplots of age-standardized rates of selected cancers as a function of tobacco exposure, Figure S4. Pannelled scatterplots of age-standardized rates of selected cancers as a function of alcohol use disorder incidence, Figure S5. Pannelled scatterplots of age-standardized rates of selected cancers as a function of Δ9THC exposure, Figure S6. Time-aggregated rates of selected cancers in highest and lowest tobacco exposure quintiles, Figure S7. Time-aggregated rates of selected cancers in highest and lowest alcohol use disorder incidence quintuiles, Figure S8. Time-aggregated rates of selected cancers in highest and lowest Δ9THC exposure quintiles, Figure S9. Time-aggregated rates of selected cancers in highest and lowest Δ8THC exposure quintiles, Figure S10. Graphical summary of inverse probability weighted additive panel models by covariate. (A) numbers of cancers identified, (B) total negative P-value of exponents and (C) total minimum E-values, Figure S11. Graphical summary of inverse probability weighted interactive panel models at two years lag by covariate. (A) numbers of cancers identified, (B) total negative P-value of exponents and (C) total minimum E-values, Figure S12. Heatmap of substance martginal effects in additive panel model by tumour type, Figure S13. Heatmap of substance martginal effects in interactive panel model at two years of lag by tumour type, Figure S14. Heatmap of substance martginal effects in interactive panel model at four years of lag by tumour type. Tables S1–S20.

**Author Contributions:** A.S.R. assembled the data, designed, and conducted the analyses, and wrote the first manuscript draft. G.K.H. provided technical and logistic support, co-wrote the paper, assisted with gaining ethical approval, provided advice on the manuscript preparation, and general guidance in conducting the study. A.S.R. had the idea for the article, performed the literature search, wrote the first draft, and is the guarantor for the article. All authors have read and agreed to the published version of the manuscript.

**Funding:** This research received no external funding.

**Institutional Review Board Statement:** Ethics Approval and Consent to Participate, The Human Research Ethics Committee of the University of Western Australia provided ethical approval for the study to be undertaken, dated 24 September 2021 (No. RA/4/20/4724).

**Informed Consent Statement:** Not applicable.

**Data Availability Statement:** All data generated or analyzed during this study are included in this published article and its Supplementary Materials files. Data, along with the relevant R code, have been made publicly available on the Mendeley Database Repository and can be accessed from this URL, doi:10.17632/vd6mt5r5jm.1.

**Acknowledgments:** All authors had full access to all of the data in the study and take responsibility for the integrity of the data and the accuracy of the data analysis.

**Conflicts of Interest:** The authors declare no conflict of interest.

## References


1. Babalonis, S.; Raup-Konsavage, W.M.; Akpunonu, P.D.; Balla, A.; Vrana, K.E. Δ(8)-THC: Legal Status, Widespread Availability, and Safety Concerns. *Cannabis Cannabinoid Res.* **2021**, *6*, 362–365. [CrossRef] [PubMed]
2. National Library of Medicine. PubChem: Delta8-Tetrahydrocannabinol (Compound). Available online: https://pubchem.ncbi.nlm.nih.gov/compound/delta8-Tetrahydrocannabinol (accessed on 10 January 2022).
3. Centers for Disease Control and Prevention. Increases in Availability of Cannabis Products Containing Delta-8 THC and Reported Cases of Adverse Events. Available online: https://emergency.cdc.gov/han/2021/han00451.asp (accessed on 10 January 2022).
4. U.S. Food and Drug Administration. 5 Things to Know about Delta-8 Tetrahydrocannabinol—Delta-8 THC. Available online: https://www.fda.gov/consumers/consumer-updates/5-things-know-about-delta-8-tetrahydrocannabinol-delta-8-thc (accessed on 10 January 2022).
5. Ross, R.A.; Gibson, T.M.; Stevenson, L.A.; Saha, B.; Crocker, P.; Razdan, R.K.; Pertwee, R.G. Structural determinants of the partial agonist-inverse agonist properties of 6′-azidohex-2′-yne-delta8-tetrahydrocannabinol at cannabinoid receptors. *Br. J. Pharmacol.* **1999**, *128*, 735–743. [CrossRef] [PubMed]
6. Thompson, G.R.; Rosenkrantz, H.; Schaeppi, U.H.; Braude, M.C. Comparison of acute oral toxicity of cannabinoids in rats, dogs and monkeys. *Toxicol. Appl. Pharmacol.* **1973**, *25*, 363–372. [CrossRef]
7. Leuchtenberger, C.; Leuchtenberger, R. Morphological and cytochemical effects of marijuana cigarette smoke on epithelioid cells of lung explants from mice. *Nature* **1971**, *234*, 227–229. [CrossRef]
8. Leuchtenberger, C.; Leuchtenberger, R.; Schneider, A. Effects of marijuana and tobacco smoke on human lung physiology. *Nature* **1973**, *241*, 137–139. [CrossRef]
9. Stenchever, M.A.; Kunysz, T.J.; Allen, M.A. Chromosome breakage in users of marihuana. *Am. J. Obstet. Gynecol.* **1974**, *118*, 106–113. [CrossRef]
10. Zimmerman, A.M.; Zimmerman, S.; Raj, A.Y. Effects of Cannabinoids on Spermatogensis in Mice. In *Marijuana and Medicine*, 1st ed.; Nahas, G.G., Sutin, K.M., Harvey, D.J., Agurell, S., Eds.; Humana Press: Totowa, NJ, USA, 1999; Volume 1, pp. 347–358.
11. Morishima, A.; Henrich, R.T.; Jayaraman, J.; Nahas, G.G. Hypoploid metaphases in cultured lymphocytes of marihuana smokers. *Adv. Biosci.* **1978**, *22–23*, 371–376.
12. Henrich, R.T.; Nogawa, T.; Morishima, A. In vitro induction of segregational errors of chromosomes by natural cannabinoids in normal human lymphocytes. *Environ. Mutagenesis* **1980**, *2*, 139–147. [CrossRef]
13. Russo, C.; Ferk, F.; Mišík, M.; Ropek, N.; Nersesyan, A.; Mejri, D.; Holzmann, K.; Lavorgna, M.; Isidori, M.; Knasmüller, S. Low doses of widely consumed cannabinoids (cannabidiol and cannabidivarin) cause DNA damage and chromosomal aberrations in human-derived cells. *Arch. Toxicol.* **2019**, *93*, 179–188. [CrossRef]
14. Szutorisz, H.; DiNieri, J.A.; Sweet, E.; Egervari, G.; Michaelides, M.; Carter, J.M.; Ren, Y.; Miller, M.L.; Blitzer, R.D.; Hurd, Y.L. Parental THC exposure leads to compulsive heroin-seeking and altered striatal synaptic plasticity in the subsequent generation. *Neuropsychopharmacology* **2014**, *39*, 1315–1323. [CrossRef]
15. Szutorisz, H.; Hurd, Y.L. Epigenetic Effects of Cannabis Exposure. *Biol. Psychiatry* **2016**, *79*, 586–594. [CrossRef] [PubMed]
16. Watson, C.T.; Szutorisz, H.; Garg, P.; Martin, Q.; Landry, J.A.; Sharp, A.J.; Hurd, Y.L. Genome-Wide DNA Methylation Profiling Reveals Epigenetic Changes in the Rat Nucleus Accumbens Associated with Cross-Generational Effects of Adolescent THC Exposure. *Neuropsychopharmacology* **2015**, *40*, 2993–3005. [CrossRef] [PubMed]
17. Bartova, A.; Birmingham, M.K. Effect of delta9-tetrahydrocannabinol on mitochondrial NADH-oxidase activity. *J. Biol. Chem.* **1976**, *251*, 5002–5006. [CrossRef]
18. Benard, G.; Massa, F.; Puente, N.; Lourenco, J.; Bellocchio, L.; Soria-Gomez, E.; Matias, I.; Delamarre, A.; Metna-Laurent, M.; Cannich, A.; et al. Mitochondrial CB(1) receptors regulate neuronal energy metabolism. *Nat. Neurosci.* **2012**, *15*, 558–564. [CrossRef] [PubMed]
19. Hebert-Chatelain, E.; Desprez, T.; Serrat, R.; Bellocchio, L.; Soria-Gomez, E.; Busquets-Garcia, A.; Pagano Zottola, A.C.; Delamarre, A.; Cannich, A.; Vincent, P.; et al. A cannabinoid link between mitochondria and memory. *Nature* **2016**, *539*, 555–559. [CrossRef]
20. Hebert-Chatelain, E.; Reguero, L.; Puente, N.; Lutz, B.; Chaouloff, F.; Rossignol, R.; Piazza, P.V.; Benard, G.; Grandes, P.; Marsicano, G. Cannabinoid control of brain bioenergetics: Exploring the subcellular localization of the CB1 receptor. *Mol. Metab.* **2014**, *3*, 495–504. [CrossRef]
21. Mahoney, J.M.; Harris, R.A. Effect of 9-tetrahydrocannabinol on mitochondrial processes. *Biochem. Pharmacol.* **1972**, *21*, 1217–1226. [CrossRef]
22. Callaghan, R.C.; Allebeck, P.; Akre, O.; McGlynn, K.A.; Sidorchuk, A. Cannabis Use and Incidence of Testicular Cancer: A 42-Year Follow-up of Swedish Men between 1970 and 2011. *Cancer Epidemiol. Biomark. Prev.* **2017**, *26*, 1644–1652. [CrossRef]
23. Daling, J.R.; Doody, D.R.; Sun, X.; Trabert, B.L.; Weiss, N.S.; Chen, C.; Biggs, M.L.; Starr, J.R.; Dey, S.K.; Schwartz, S.M. Association of marijuana use and the incidence of testicular germ cell tumors. *Cancer* **2009**, *115*, 1215–1223. [CrossRef]
24. Lacson, J.C.; Carroll, J.D.; Tuazon, E.; Castelao, E.J.; Bernstein, L.; Cortessis, V.K. Population-based case-control study of recreational drug use and testis cancer risk confirms an association between marijuana use and nonseminoma risk. *Cancer* **2012**, *118*, 5374–5383. [CrossRef]
25. Trabert, B.; Sigurdson, A.J.; Sweeney, A.M.; Strom, S.S.; McGlynn, K.A. Marijuana use and testicular germ cell tumors. *Cancer* **2011**, *117*, 848–853. [CrossRef] [PubMed]
26. Reece, A.S. Chronic toxicology of cannabis. *Clin. Toxicol.* **2009**, *47*, 517–524. [CrossRef] [PubMed]

27. Reece, A.S.; Hulse, G.K. Epidemiological Overview of Multidimensional Chromosomal and Genome Toxicity of Cannabis Exposure in Congenital Anomalies and Cancer Development. *Sci. Rep.* **2021**, *11*, 13892–13912. [CrossRef] [PubMed]
28. Reece, A.S.; Hulse, G.K. Cannabinoid exposure as a major driver of pediatric acute lymphoid Leukaemia rates across the USA: Combined geospatial, multiple imputation and causal inference study. *BMC Cancer* **2021**, *21*, 984–1017. [CrossRef]
29. Grobner, S.N.; Worst, B.C.; Weischenfeldt, J.; Buchhalter, I.; Kleinheinz, K.; Rudneva, V.A.; Johann, P.D.; Balasubramanian, G.P.; Segura-Wang, M.; Brabetz, S.; et al. The landscape of genomic alterations across childhood cancers. *Nature* **2018**, *555*, 321–327. [CrossRef]
30. Ma, X.; Liu, Y.; Liu, Y.; Alexandrov, L.B.; Edmonson, M.N.; Gawad, C.; Zhou, X.; Li, Y.; Rusch, M.C.; Easton, J.; et al. Pan-cancer genome and transcriptome analyses of 1699 paediatric leukaemias and solid tumours. *Nature* **2018**, *555*, 371–376. [CrossRef]
31. Nahas, G.G.; Morishima, A.; Desoize, B. Effects of cannabinoids on macromolecular synthesis and replication of cultured lymphocytes. *Fed. Proc.* **1977**, *36*, 1748–1752.
32. McClean, D.K.; Zimmerman, A.M. Action of delta 9-tetrahydrocannabinol on cell division and macromolecular synthesis in division-synchronized protozoa. *Pharmacology* **1976**, *14*, 307–321. [CrossRef]
33. Zimmerman, A.M.; Stich, H.; San, R. Nonmutagenic action of cannabinoids in vitro. *Pharmacology* **1978**, *16*, 333–343. [CrossRef]
34. Thomas, J.; Tilak, S.; Zimmerman, S.; Zimmerman, A.M. Action of delta 9-tetrahydrocannabinol on the pool of acid soluble nucleotides. *Cytobios* **1984**, *40*, 71–85.
35. Tahir, S.K.; Zimmerman, A.M. Influence of marihuana on cellular structures and biochemical activities. *Pharmacol. Biochem. Behav.* **1991**, *40*, 617–623. [CrossRef]
36. Carchman, R.A.; Harris, L.S.; Munson, A.E. The inhibition of DNA synthesis by cannabinoids. *Cancer Res.* **1976**, *36*, 95–100. [PubMed]
37. Friedman, M.A. In vivo effects of cannabinoids on macromolecular biosynthesis in Lewis lung carcinomas. *Cancer Biochem. Biophys.* **1977**, *2*, 51–54. [PubMed]
38. Tucker, A.N.; Friedman, M.A. Effects of cannabinoids on L1210 murine leukemia. 1. Inhibition of DNA synthesis. *Res. Commun. Chem. Pathol. Pharmacol.* **1977**, *17*, 703–714.
39. Krishnamurthy, M.; Gurley, S.; Moore, B.M., 2nd. Exploring the substituent effects on a novel series of C1′-dimethyl-aryl Delta8-tetrahydrocannabinol analogs. *Bioorganic Med. Chem.* **2008**, *16*, 6489–6500. [CrossRef]
40. Semlali, A.; Beji, S.; Ajala, I.; Rouabhia, M. Effects of tetrahydrocannabinols on human oral cancer cell proliferation, apoptosis, autophagy, oxidative stress, and DNA damage. *Arch. Oral Biol.* **2021**, *129*, 105200. [CrossRef]
41. Nahas, G.G. *Cannabis Physiopathology Epidemiology Detection*; CRC Press Revivals: Boca Raton, FL, USA, 1990; Volume 1.
42. Nahas, G.G. *Keep off the Grass*; Eriksson, P.S., Ed.; Elsevier: Middlebury, VT, USA, 1990; Volume 1.
43. Huang, H.F.S.; Nahas, G.G.; Hembree, W.C. Effects of Marijuana Inhalation on Spermatogenesis of the Rat. In *Marijuana in Medicine*; Nahas, G.G., Sutin, K.M., Harvey, D.J., Agurell, S., Eds.; Human Press: Totowa, NJ, USA, 1999; Volume 1, pp. 359–366.
44. Reece, A.S.; Hulse, G.K. Cannabis Teratology Explains Current Patterns of Coloradan Congenital Defects: The Contribution of Increased Cannabinoid Exposure to Rising Teratological Trends. *Clin. Pediatrics* **2019**, *58*, 1085–1123. [CrossRef]
45. Reece, A.S.; Hulse, G.K. Cannabis in Pregnancy—Rejoinder, Exposition and Cautionary Tales. *Psychiatr. Times* **2020**, *37*.
46. Reece, A.S.; Hulse, G.K. Broad Spectrum epidemiological contribution of cannabis and other substances to the teratological profile of northern New South Wales: Geospatial and causal inference analysis. *BMC Pharmacol. Toxicol.* **2020**, *21*, 75–103. [CrossRef]
47. Reece, A.S.; Hulse, G.K. Canadian Cannabis Consumption and Patterns of Congenital Anomalies: An Ecological Geospatial Analysis. *J. Addict. Med.* **2020**, *14*, e195–e210. [CrossRef]
48. Lu, Y.; Brommer, B.; Tian, X.; Krishnan, A.; Meer, M.; Wang, C.; Vera, D.L.; Zeng, Q.; Yu, D.; Bonkowski, M.S.; et al. Reprogramming to recover youthful epigenetic information and restore vision. *Nature* **2020**, *588*, 124–129. [CrossRef] [PubMed]
49. National Program of Cancer Registries and Surveillance, Epidemiology, and End Results SEER*Stat Database: NPCR and SEER Incidence—U.S. Cancer Statistics Public Use Research Database, 2019 Submission (2001–2017), United States Department of Health and Human Services, Centers for Disease Control and Prevention and National Cancer Institute. Released June 2020. Available online: www.cdc.gov/cancer/public-use (accessed on 10 January 2022).
50. National Survey of Drug Use and Health 2018, NSDUH. Available online: https://www.samhsa.gov/data/all-reports (accessed on 10 January 2022).
51. Tidycensus: Load US Census Boundary and Attribute Data as 'Tidyverse' and 'sf'-Ready Data Frames. Available online: https://www.r-pkg.org/pkg/tidycensus (accessed on 10 January 2022).
52. ElSohly, M.A.; Mehmedic, Z.; Foster, S.; Gon, C.; Chandra, S.; Church, J.C. Changes in Cannabis Potency over the Last 2 Decades (1995–2014): Analysis of Current Data in the United States. *Biol. Psychiatry* **2016**, *79*, 613–619. [CrossRef] [PubMed]
53. Chandra, S.; Radwan, M.M.; Majumdar, C.G.; Church, J.C.; Freeman, T.P.; ElSohly, M.A. New trends in cannabis potency in USA and Europe during the last decade (2008–2017). *Eur. Arch. Psychiatry Clin. Neurosci.* **2019**, *269*, 5–15. [CrossRef] [PubMed]
54. ElSohly, M.A.; Ross, S.A.; Mehmedic, Z.; Arafat, R.; Yi, B.; Banahan, B.F., 3rd. Potency trends of delta9-THC and other cannabinoids in confiscated marijuana from 1980–1997. *J. Forensic Sci.* **2000**, *45*, 24–30. [CrossRef] [PubMed]
55. Wickham, H.; Averick, M.; Bryan, J.; Chang, W.; McGowan, L.D.; Francios, R.; Groelmund, G.; Hayes, A.; Henry, L.; Hester, J.; et al. Welcome to the Tidyverse. *J. Open Source Softw.* **2019**, *4*, 1686–1691. [CrossRef]
56. Pebesma, E. Simple Features for R: Standardized Support for Spatial Vector Data. *R J.* **2018**, *10*, 439–446. [CrossRef]

57. Warnes, G.R.; Bolker, B.; Bonebakker, L.; Gentleman, R.; Huber, W.; Liaw, A.; Lumley, T.; Maechler, M.; Magnusson, A.; Moeller, S.; et al. *gplots: Various R Programming Tools for Plotting Data*; R Package Version 3.1.1; R Foundation: Vienna, Austria, 2020.
58. Stevenson, M.; Sergeant, E.; Nunes, T.; Heuer, C.; Marshall, J.; Sanchez, J.; Thornton, R.; Reiczigel, J.; Robison-Cox, J.; Sebastiani, P.; et al. epiR: Tools for the Analysis of Epidemiological Data. Available online: https://fvas.unimelb.edu.au/research/groups/veterinary-epidemiology-melbourne (accessed on 10 January 2022).
59. Croissant, Y.; Millo, G.; Tappe, K.; Toomet, O.; Kleiber, C.; Zeileis, A.; Henningsen, A.; Andronic, L.; Schoenfelder, N. Package 'plm'. Available online: https://cran.r-project.org/web/packages/plm/plm.pdf (accessed on 10 January 2022).
60. Wal, W.; Geskus, R. ipw: An R Package for Inverse Probability Weighting. *J. Stat. Softw.* **2011**, *43*, 1–23. [CrossRef]
61. VanderWeele, T.J.; Ding, P. Sensitivity Analysis in Observational Research: Introducing the E-Value. *Ann. Intern. Med.* **2017**, *167*, 268–274. [CrossRef]
62. VanderWeele, T.J.; Mathur, M.B. Commentary: Developing best-practice guidelines for the reporting of E-values. *Int. J. Epidemiol.* **2020**, *49*, 1495–1497. [CrossRef]
63. Mathur, M. Package 'EValue'. Available online: https://cran.r-project.org/web/packages/EValue/index.html (accessed on 10 January 2022).
64. VanderWeele, T.J.; Ding, P.; Mathur, M. Technical Considerations in the Use of the E-Value. *J. Causal Inference* **2019**, *7*, 1–11. [CrossRef]
65. Pearl, J.; Mackaenzie, D. *The Book of Why: The New Science of Cause and Effect*; Basic Books: New York, NY, USA, 2019; Volume 1.
66. Leeper, T.J. *Margins: Marginal Effects for Model Objects*; R Package Version 0.3.26; R Foundation: Vienna, Austria, 2021; pp. 1–36.
67. Robinson, D.; Hayes, A.; Couch, S. Broom: Convert Statistical Objects into Tidy Tibbles. Available online: https://CRAN.R-project.org/package=broom (accessed on 10 January 2022).
68. Hill, A.B. The Environment and Disease: Association or Causation? *Proc. R Soc. Med.* **1965**, *58*, 295–300. [CrossRef] [PubMed]
69. Jakubovič, A.; McGeer, P.L.; Fitzsimmons, R.C. Effects of Δ9-tetrahydrocannabinol and ethanol on body weight protein and nucleic acid synthesis in chick embryos. *J. Toxicol. Environ. Health* **1976**, *1*, 441–447. [CrossRef] [PubMed]
70. Wang, J.; Yuan, W.; Li, M.D. Genes and pathways co-associated with the exposure to multiple drugs of abuse, including alcohol, amphetamine/methamphetamine, cocaine, marijuana, morphine, and/or nicotine: A review of proteomics analyses. *Mol. Neurobiol.* **2011**, *44*, 269–286. [CrossRef] [PubMed]
71. Murphy, S.K.; Itchon-Ramos, N.; Visco, Z.; Huang, Z.; Grenier, C.; Schrott, R.; Acharya, K.; Boudreau, M.H.; Price, T.M.; Raburn, D.J.; et al. Cannabinoid exposure and altered DNA methylation in rat and human sperm. *Epigenetics* **2018**, *13*, 1208–1221. [CrossRef] [PubMed]
72. DiNieri, J.A.; Wang, X.; Szutorisz, H.; Spano, S.M.; Kaur, J.; Casaccia, P.; Dow-Edwards, D.; Hurd, Y.L. Maternal cannabis use alters ventral striatal dopamine D2 gene regulation in the offspring. *Biol. Psychiatry* **2011**, *70*, 763–769. [CrossRef]
73. Levin, E.D.; Hawkey, A.B.; Hall, B.J.; Cauley, M.; Slade, S.; Yazdani, E.; Kenou, B.; White, H.; Wells, C.; Rezvani, A.H.; et al. Paternal THC exposure in rats causes long-lasting neurobehavioral effects in the offspring. *Neurotoxicol. Teratol.* **2019**, *74*, 106806. [CrossRef]
74. Holloway, Z.R.; Hawkey, A.B.; Pippin, E.; White, H.; Wells, C.; Kenou, B.; Rezvani, A.H.; Murphy, S.K.; Levin, E.D. Paternal factors in neurodevelopmental toxicology: THC exposure of male rats causes long-lasting neurobehavioral effects in their offspring. *Neurotoxicology* **2020**, *78*, 57–63. [CrossRef]
75. Schrott, R.; Murphy, S.K.; Modliszewski, J.L.; King, D.E.; Hill, B.; Itchon-Ramos, N.; Raburn, D.; Price, T.; Levin, E.D.; Vandrey, R.; et al. Refraining from use diminishes cannabis-associated epigenetic changes in human sperm. *Environ. Epigenetics* **2021**, *7*, dvab009. [CrossRef]
76. Shen, H.; Shih, J.; Hollern, D.P.; Wang, L.; Bowlby, R.; Tickoo, S.K.; Thorsson, V.; Mungall, A.J.; Newton, Y.; Hegde, A.M.; et al. Integrated Molecular Characterization of Testicular Germ Cell Tumors. *Cell Rep.* **2018**, *23*, 3392–3406. [CrossRef]
77. Malouf, C.; Ottersbach, K. Molecular processes involved in B cell acute lymphoblastic leukaemia. *Cell Mol. Life Sci.* **2018**, *75*, 417–446. [CrossRef]
78. Reece, A.S.; Hulse, G.K. Geotemporospatial and Causal Inferential Epidemiological Overview and Survey of USA Cannabis, Cannabidiol and Cannabinoid Genotoxicity Expressed in Cancer Incidence 2003–2017: Part 1—Continuous Bivariate Analysis. *Arch. Public Health* **2022**, *80*, 99–133. [CrossRef] [PubMed]
79. Reece, A.S.; Hulse, G.K. Geotemporospatial and Causal Inferential Epidemiological Overview and Survey of USA Cannabis, Cannabidiol and Cannabinoid Genotoxicity Expressed in Cancer Incidence 2003–2017: Part 2—Categorical Bivariate Analysis and Attributable Fractions. *Arch. Public Health* **2022**, *80*, 100–135. [CrossRef] [PubMed]
80. Reece, A.S.; Hulse, G.K. Geotemporospatial and Causal Inferential Epidemiological Overview and Survey of USA Cannabis, Cannabidiol and Cannabinoid Genotoxicity Expressed in Cancer Incidence 2003–2017: Part 3—Spatiotemporal, Multivariable and Causal Inferential Pathfinding and Exploratory Analyses of Prostate and Ovarian Cancers. *Arch. Public Health* **2022**, *80*, 100–136. [CrossRef] [PubMed]
81. Reece, A.S.; Hulse, G.K. Geotemporospatial and causal inference epidemiological analysis of US survey and overview of cannabis, cannabidiol and cannabinoid genotoxicity in relation to congenital anomalies 2001–2015. *BMC Pediatrics* **2022**, *22*, 47–124. [CrossRef] [PubMed]
82. Szutorisz, H.; Hurd, Y.L. High times for cannabis: Epigenetic imprint and its legacy on brain and behavior. *Neurosci. Biobehav. Rev.* **2018**, *85*, 93–101. [CrossRef] [PubMed]

83. Ellis, R.J.; Bara, A.; Vargas, C.A.; Frick, A.L.; Loh, E.; Landry, J.; Uzamere, T.O.; Callens, J.E.; Martin, Q.; Rajarajan, P.; et al. Prenatal Δ(9)-Tetrahydrocannabinol Exposure in Males Leads to Motivational Disturbances Related to Striatal Epigenetic Dysregulation. *Biol. Psychiatry* 2021, *in press*. [CrossRef]
84. Schrott, R.; Acharya, K.; Itchon-Ramos, N.; Hawkey, A.B.; Pippen, E.; Mitchell, J.T.; Kollins, S.H.; Levin, E.D.; Murphy, S.K. Cannabis use is associated with potentially heritable widespread changes in autism candidate gene DLGAP2 DNA methylation in sperm. *Epigenetics* **2020**, *15*, 161–173. [CrossRef]
85. Zimmerman, A.M.; Raj, A.Y. Influence of cannabinoids on somatic cells in vivo. *Pharmacology* **1980**, *21*, 277–287. [CrossRef]
86. Zimmerman, A.M.; Zimmerman, S. Cytogenetic Studies of Cannabinoid Effects. In *Genetic and Perinatal Effects of Abused Substances*; Braude, M.C., Zimmerman, A.M., Eds.; Academic Press Inc., Harcourt, Brace Jovanovich: New York, NY, USA, 1987; Volume 1, pp. 95–112.
87. Zimmerman, S.; Zimmerman, A.M. Genetic effects of marijuana. *Int. J. Addict.* **1990**, *25*, 19–33. [CrossRef]
88. Tahir, S.K.; Trogadis, J.E.; Stevens, J.K.; Zimmerman, A.M. Cytoskeletal organization following cannabinoid treatment in undifferentiated and differentiated PC12 cells. *Biochem. Cell Biol.* **1992**, *70*, 1159–1173. [CrossRef]
89. Parker, S.J.; Zuckerman, B.S.; Zimmermann, A.M. The Effects of Maternal Marijuana Use during Pregnancy on Fetal Growth. In *Marijuana in Medicine*; Nahas, G.G., Sutin, K.M., Harvey, D.J., Agurell, S., Eds.; Humana Press: Totowa, NJ, USA, 1999; Volume 1, pp. 461–468.
90. Cozens, D.D.; Clark, R.; Palmer, A.K.; Hardy, N.; Nahas, G.G.; Harvey, D.J. The effect of a crude marihuana extract on embryonic and foetal development of the rabbit. *Adv. Biosci.* **1978**, *22–23*, 469–477.
91. Cozens, D.D.; Nahas, G.G.; Harvey, D. Prenatal Exposure to Cannabis and Fetal Development. In *Marijuana in Medicine*; Nahas, G.G., Sutin, K.M., Harvey, D.J., Agurell, S., Eds.; Humana Press: Totowa, NJ, USA, 1999; Volume 1, pp. 431–440.
92. Khwaja, A.; Bjorkholm, M.; Gale, R.E.; Levine, R.L.; Jordan, C.T.; Ehninger, G.; Bloomfield, C.D.; Estey, E.; Burnett, A.; Cornelissen, J.J.; et al. Acute myeloid leukaemia. *Nat. Rev. Dis. Primers* **2016**, *2*, 16010. [CrossRef] [PubMed]
93. Gurney, J.; Shaw, C.; Stanley, J.; Signal, V.; Sarfati, D. Cannabis exposure and risk of testicular cancer: A systematic review and meta-analysis. *BMC Cancer* **2015**, *15*, 897–906. [CrossRef] [PubMed]
94. Reece, A.S.; Hulse, G.K. Causal inference multiple imputation investigation of the impact of cannabinoids and other substances on ethnic differentials in US testicular cancer incidence. *BMC Pharmacol. Toxicol.* **2021**, *22*, 40–71. [CrossRef]
95. Reece, A.S.; Hulse, G.K. Cannabinoid- and Substance-Relationships of European Congenital Anomaly Patterns: A Space-Time Panel Regression and Causal Inferential Study. *Environ. Epigenetics* **2022**, *8*, dvab015. [CrossRef]
96. Reece, A.S.; Hulse, G.K. Cannabis Genotoxicity and Cancer Incidence: A Highly Concordant Synthesis of European and USA Datasets. In *Cannabis, Cannabinoids and Endocannabinoids*; Preedy, V., Patel, V., Eds.; Elsevier: London, UK, 2022; Volume 1, *in press*.
97. Reece, A.S.; Hulse, G.K. Cannabinoid Genotoxicity and Congenital Anomalies: A Convergent Synthesis of European and USA Datasets. In *Cannabis, Cannabinoids and Endocannabinoids*; Preedy, V., Patel, V., Eds.; Elsevier: London, UK, 2022; Volume 1, *in press*.
98. Morishima, A. Effects of cannabis and natural cannabinoids on chromosomes and ova. *NIDA Res. Monogr.* **1984**, *44*, 25–45.
99. McClintock, B. The Production of Homozygous Deficient Tissues with Mutant Characteristics by Means of the Aberrant Mitotic Behavior of Ring-Shaped Chromosomes. *Genetics* **1938**, *23*, 315–376. [CrossRef]
100. McClintock, B. The Stability of Broken Ends of Chromosomes in Zea Mays. *Genetics* **1941**, *26*, 234–282. [CrossRef]
101. Forrester, M.B.; Merz, R.D. Risk of selected birth defects with prenatal illicit drug use, Hawaii, 1986–2002. *J. Toxicol. Environ. Health* **2007**, *70*, 7–18. [CrossRef]
102. Leuchtenberger, C.; Leuchtenberger, R.; Ritter, U.; Inui, N. Effects of marijuana and tobacco smoke on DNA and chromosomal complement in human lung explants. *Nature* **1973**, *242*, 403–404. [CrossRef]
103. Hall, W.; Degenhardt, L. Adverse health effects of non-medical cannabis use. *Lancet* **2009**, *374*, 1383–1391. [CrossRef]
104. Reece, A.S.; Hulse, G.K. Chromothripsis and epigenomics complete causality criteria for cannabis- and addiction-connected carcinogenicity, congenital toxicity and heritable genotoxicity. *Mutat. Res.* **2016**, *789*, 15–25. [CrossRef] [PubMed]
105. Zhang, C.Z.; Spektor, A.; Cornils, H.; Francis, J.M.; Jackson, E.K.; Liu, S.; Meyerson, M.; Pellman, D. Chromothripsis from DNA damage in micronuclei. *Nature* **2015**, *522*, 179–184. [CrossRef]
106. Kuhn, J.; Dumont, S. Mammalian kinetochores count attached microtubules in a sensitive and switch-like manner. *J. Cell Biol.* **2019**, *218*, 3583–3596. [CrossRef] [PubMed]
107. Beh, T.T.; Kalitsis, P. Centromeres and Kinetochores. In *Centromeres and Kinetochores*; Black, B.E., Ed.; Springer: Philadelphia, PA, USA, 2017.
108. Beh, T.T.; Kalitsis, P. The Role of Centromere Defects in Cancer. In *Centromeres and Kinetochores*; Black, B.E., Ed.; Springer: Philadelphia, PA, USA, 2017; Volume 1, pp. 1–554.
109. Black, B.E. Preface to: Centromeres and Kinetochores. In *Centromeres and Kinetochores*; Black, B.E., Ed.; Springer: Cham, Switzerland, 2017; Volume 1, pp. v–viii.
110. Corbett, K.D. Molecular Mechanisms of Spindle Assembly Checkpoint Activation and Silencing. In *Centromeres and Kinetochores*; Black, B.E., Ed.; Springer: Philadelphia, PA, USA, 2017; Volume 1, pp. 1–554.
111. French, B.T.; Straight, A.F. The Power of Xenopus Egg Extract for Reconstitution of Centromere and Kinetochore Function. In *Centromeres and Kinetochores*; Black, B.E., Ed.; Springer: Philadelphia, PA, USA, 2017; Volume 1, pp. 1–554.
112. Hara, M.; Fukagawa, T. Critical Foundation of the Kinetochore: The Constitutive Centromere—Associated Network (CCAN). In *Centromeres and Kinetochores*; Black, B.E., Ed.; Springer: Philadelphia, PA, USA, 2017; Volume 1, pp. 1–554.

113. Dong, Q.; Liu, X.L.; Wang, X.H.; Zhao, Y.; Chen, Y.H.; Li, F. Ccp1-Ndc80 switch at the N terminus of CENP-T regulates kinetochore assembly. *Proc. Natl. Acad. Sci. USA* **2021**, *118*, e2104459118. [CrossRef] [PubMed]
114. Mellone, B.G.; Fachinetti, D. Diverse mechanisms of centromere specification. *Curr. Biol.* **2021**, *31*, R1491–R1504. [CrossRef]
115. Ryu, H.Y.; Hochstrasser, M. Histone sumoylation and chromatin dynamics. *Nucleic Acids Res.* **2021**, *49*, 6043–6052. [CrossRef]
116. Gowran, A.; Murphy, C.E.; Campbell, V.A. Delta(9)-tetrahydrocannabinol regulates the p53 post-translational modifiers Murine double minute 2 and the Small Ubiquitin MOdifier protein in the rat brain. *FEBS Lett.* **2009**, *583*, 3412–3418. [CrossRef]
117. Attia, S.M.; Al-Khalifa, M.K.; Al-Hamamah, M.A.; Alotaibi, M.R.; Attia, M.S.M.; Ahmad, S.F.; Ansari, M.A.; Nadeem, A.; Bakheet, S.A. Vorinostat is genotoxic and epigenotoxic in the mouse bone marrow cells at the human equivalent doses. *Toxicology* **2020**, *441*, 152507. [CrossRef]
118. Ben Yamin, B.; Ahmed-Seghir, S.; Tomida, J.; Despras, E.; Pouvelle, C.; Yurchenko, A.; Goulas, J.; Corre, R.; Delacour, Q.; Droin, N.; et al. DNA polymerase zeta contributes to heterochromatin replication to prevent genome instability. *EMBO J.* **2021**, *40*, e104543. [CrossRef]
119. Cheloshkina, K.; Poptsova, M. Comprehensive analysis of cancer breakpoints reveals signatures of genetic and epigenetic contribution to cancer genome rearrangements. *PLoS Comput. Biol.* **2021**, *17*, e1008749. [CrossRef] [PubMed]
120. García Fernández, F.; Lemos, B.; Khalil, Y.; Batrin, R.; Haber, J.E.; Fabre, E. Modified chromosome structure caused by phosphomimetic H2A modulates the DNA damage response by increasing chromatin mobility in yeast. *J. Cell Sci.* **2021**, *134*, jcs258500. [CrossRef] [PubMed]
121. George, J.; Lim, J.S.; Jang, S.J.; Cun, Y.; Ozretić, L.; Kong, G.; Leenders, F.; Lu, X.; Fernández-Cuesta, L.; Bosco, G.; et al. Comprehensive genomic profiles of small cell lung cancer. *Nature* **2015**, *524*, 47–53. [CrossRef] [PubMed]
122. Harrod, A.; Lane, K.A.; Downs, J.A. The role of the SWI/SNF chromatin remodelling complex in the response to DNA double strand breaks. *DNA Repair* **2020**, *93*, 102919. [CrossRef] [PubMed]
123. He, Y.; Ren, J.; Xu, X.; Ni, K.; Schwader, A.; Finney, R.; Wang, C.; Sun, L.; Klarmann, K.; Keller, J.; et al. Lsh/HELLS is required for B lymphocyte development and immunoglobulin class switch recombination. *Proc. Natl. Acad. Sci. USA* **2020**, *117*, 20100–20108. [CrossRef]
124. Jamsen, J.A.; Sassa, A.; Perera, L.; Shock, D.D.; Beard, W.A.; Wilson, S.H. Structural basis for proficient oxidized ribonucleotide insertion in double strand break repair. *Nat. Commun.* **2021**, *12*, 5055. [CrossRef]
125. Llorens-Agost, M.; Ensminger, M.; Le, H.P.; Gawai, A.; Liu, J.; Cruz-García, A.; Bhetawal, S.; Wood, R.D.; Heyer, W.D.; Löbrich, M. POLθ-mediated end joining is restricted by RAD52 and BRCA2 until the onset of mitosis. *Nat. Cell Biol.* **2021**, *23*, 1095–1104. [CrossRef]
126. Mir, U.S.; Bhat, A.; Mushtaq, A.; Pandita, S.; Altaf, M.; Pandita, T.K. Role of histone acetyltransferases MOF and Tip60 in genome stability. *DNA Repair* **2021**, *107*, 103205. [CrossRef]
127. Shoeb, M.; Meier, H.C.S.; Antonini, J.M. Telomeres in toxicology: Occupational health. *Pharmacol. Ther.* **2021**, *220*, 107742. [CrossRef]
128. Tsai, L.J.; Lopezcolorado, F.W.; Bhargava, R.; Mendez-Dorantes, C.; Jahanshir, E.; Stark, J.M. RNF8 has both KU-dependent and independent roles in chromosomal break repair. *Nucleic Acids Res.* **2020**, *48*, 6032–6052. [CrossRef]
129. Vasilyeva, T.A.; Marakhonov, A.V.; Sukhanova, N.V.; Kutsev, S.I.; Zinchenko, R.A. Preferentially Paternal Origin of De Novo 11p13 Chromosome Deletions Revealed in Patients with Congenital Aniridia and WAGR Syndrome. *Genes* **2020**, *11*, 812. [CrossRef] [PubMed]
130. Yamazoe, T.; Mori, T.; Yoshio, S.; Kanto, T. Hepatocyte ploidy and pathological mutations in hepatocellular carcinoma: Impact on oncogenesis and therapeutics. *Glob. Health Med.* **2020**, *2*, 273–281. [CrossRef] [PubMed]
131. Ali, S.; Zhang, T.; Lambing, C.; Wang, W.; Zhang, P.; Xie, L.; Wang, J.; Khan, N.; Zhang, Q. Loss of chromatin remodeler DDM1 causes segregation distortion in *Arabidopsis thaliana*. *Planta* **2021**, *254*, 107. [CrossRef]
132. Alonso-Ramos, P.; Álvarez-Melo, D.; Strouhalova, K.; Pascual-Silva, C.; Garside, G.B.; Arter, M.; Bermejo, T.; Grigaitis, R.; Wettstein, R.; Fernández-Díaz, M.; et al. The Cdc14 Phosphatase Controls Resolution of Recombination Intermediates and Crossover Formation during Meiosis. *Int. J. Mol. Sci.* **2021**, *22*, 9811. [CrossRef] [PubMed]
133. Arrieta, M.; Macaulay, M.; Colas, I.; Schreiber, M.; Shaw, P.D.; Waugh, R.; Ramsay, L. An Induced Mutation in HvRECQL4 Increases the Overall Recombination and Restores Fertility in a Barley HvMLH3 Mutant Background. *Front. Plant Sci.* **2021**, *12*, 706560. [CrossRef] [PubMed]
134. Gutiérrez Pinzón, Y.; González Kise, J.K.; Rueda, P.; Ronceret, A. The Formation of Bivalents and the Control of Plant Meiotic Recombination. *Front. Plant Sci.* **2021**, *12*, 717423. [CrossRef]
135. Malinovskaya, L.P.; Tishakova, K.V.; Bikchurina, T.I.; Slobodchikova, A.Y.; Torgunakov, N.Y.; Torgasheva, A.A.; Tsepilov, Y.A.; Volkova, N.A.; Borodin, P.M. Negative heterosis for meiotic recombination rate in spermatocytes of the domestic chicken Gallus gallus. *Vavilov J. Genet. Breed.* **2021**, *25*, 661–668. [CrossRef] [PubMed]
136. Maroilley, T.; Li, X.; Oldach, M.; Jean, F.; Stasiuk, S.J.; Tarailo-Graovac, M. Deciphering complex genome rearrangements in *C. elegans* using short-read whole genome sequencing. *Sci. Rep.* **2021**, *11*, 18258. [CrossRef] [PubMed]
137. Torgasheva, A.; Malinovskaya, L.; Zadesenets, K.; Shnaider, E.; Rubtsov, N.; Borodin, P. Germline-Restricted Chromosome (GRC) in Female and Male Meiosis of the Great Tit (Parus major, Linnaeus, 1758). *Front. Genet.* **2021**, *12*, 768056. [CrossRef] [PubMed]
138. Ur, S.N.; Corbett, K.D. Architecture and Dynamics of Meiotic Chromosomes. *Annu. Rev. Genet.* **2021**, *55*, 497–526. [CrossRef]

139. Ajamian, L.; Melnychuk, L.; Jean-Pierre, P.; Zaharatos, G.J. DNA Vaccine-Encoded Flagellin Can Be Used as an Adjuvant Scaffold to Augment HIV-1 gp41 Membrane Proximal External Region Immunogenicity. *Viruses* **2018**, *10*, 100. [CrossRef] [PubMed]
140. Dos Santos Rocha, A.; de Amorim, I.S.S.; Simão, T.A.; da Fonseca, A.S.; Garrido, R.G.; Mencalha, A.L. High-Resolution Melting (HRM) of Hypervariable Mitochondrial DNA Regions for Forensic Science. *J. Forensic Sci.* **2018**, *63*, 536–540. [CrossRef] [PubMed]
141. Krebs, S.J.; McBurney, S.P.; Kovarik, D.N.; Waddell, C.D.; Jaworski, J.P.; Sutton, W.F.; Gomes, M.M.; Trovato, M.; Waagmeester, G.; Barnett, S.J.; et al. Multimeric scaffolds displaying the HIV-1 envelope MPER induce MPER-specific antibodies and cross-neutralizing antibodies when co-immunized with gp160 DNA. *PLoS ONE* **2014**, *9*, e113463. [CrossRef]
142. Li, D.; Yu, A.Q.; Li, X.J.; Zhu, Y.T.; Jin, X.K.; Li, W.W.; Wang, Q. Antimicrobial activity of a novel hypervariable immunoglobulin domain-containing receptor Dscam in Cherax quadricarinatus. *Fish Shellfish Immunol.* **2015**, *47*, 766–776. [CrossRef]
143. Pogorelyy, M.V.; Minervina, A.A.; Shugay, M.; Chudakov, D.M.; Lebedev, Y.B.; Mora, T.; Walczak, A.M. Detecting T cell receptors involved in immune responses from single repertoire snapshots. *PLoS Biol.* **2019**, *17*, e3000314. [CrossRef]
144. Richter, A.; Eggenstein, E.; Skerra, A. Anticalins: Exploiting a non-Ig scaffold with hypervariable loops for the engineering of binding proteins. *FEBS Lett.* **2014**, *588*, 213–218. [CrossRef]
145. Wang, C.Y.; Fang, Y.X.; Chen, G.H.; Jia, H.J.; Zeng, S.; He, X.B.; Feng, Y.; Li, S.J.; Jin, Q.W.; Cheng, W.Y.; et al. Analysis of the CDR3 length repertoire and the diversity of T cell receptor α and β chains in swine CD4+ and CD8+ T lymphocytes. *Mol. Med. Rep.* **2017**, *16*, 75–86. [CrossRef]
146. Al-Hamamah, M.A.; Alotaibi, M.R.; Ahmad, S.F.; Ansari, M.A.; Attia, M.S.M.; Nadeem, A.; Bakheet, S.A.; As Sobeai, H.M.; Attia, S.M. Genetic and epigenetic alterations induced by the small-molecule panobinostat: A mechanistic study at the chromosome and gene levels. *DNA Repair* **2019**, *78*, 70–80. [CrossRef]
147. Bhargava, R.; Lopezcolorado, F.W.; Tsai, L.J.; Stark, J.M. The canonical non-homologous end joining factor XLF promotes chromosomal deletion rearrangements in human cells. *J. Biol. Chem.* **2020**, *295*, 125–137. [CrossRef]
148. Kelso, A.A.; Lopezcolorado, F.W.; Bhargava, R.; Stark, J.M. Distinct roles of RAD52 and POLQ in chromosomal break repair and replication stress response. *PLoS Genet.* **2019**, *15*, e1008319. [CrossRef]
149. Liu, X.; Jiang, Y.; Takata, K.I.; Nowak, B.; Liu, C.; Wood, R.D.; Hittelman, W.N.; Plunkett, W. CNDAC-Induced DNA Double-Strand Breaks Cause Aberrant Mitosis Prior to Cell Death. *Mol. Cancer Ther.* **2019**, *18*, 2283–2295. [CrossRef] [PubMed]
150. Srinivas, N.; Rachakonda, S.; Kumar, R. Telomeres and Telomere Length: A General Overview. *Cancers* **2020**, *12*, 558. [CrossRef] [PubMed]
151. Young, N.L.; Dere, R. Mechanistic insights into KDM4A driven genomic instability. *Biochem. Soc. Trans.* **2021**, *49*, 93–105. [CrossRef] [PubMed]
152. Zhang, X.; Shi, Y.; Ramesh, K.H.; Naeem, R.; Wang, Y. Karyotypic complexity, TP53 pathogenic variants, and increased number of variants on Next-Generation Sequencing are associated with disease progression in a North American Adult T-Cell Leukemia/Lymphoma cohort. *Int. J. Lab. Hematol.* **2021**, *43*, 651–657. [CrossRef]
153. Zhao, S.; Klattenhoff, A.W.; Thakur, M.; Sebastian, M.; Kidane, D. Mutation in DNA Polymerase Beta Causes Spontaneous Chromosomal Instability and Inflammation-Associated Carcinogenesis in Mice. *Cancers* **2019**, *11*, 1160. [CrossRef]
154. Bernard, E.; Nannya, Y.; Hasserjian, R.P.; Devlin, S.M.; Tuechler, H.; Medina-Martinez, J.S.; Yoshizato, T.; Shiozawa, Y.; Saiki, R.; Malcovati, L.; et al. Implications of TP53 allelic state for genome stability, clinical presentation and outcomes in myelodysplastic syndromes. *Nat. Med.* **2020**, *26*, 1549–1556. [CrossRef]
155. Brieghel, C.; Aarup, K.; Torp, M.H.; Andersen, M.A.; Yde, C.W.; Tian, X.; Wiestner, A.; Ahn, I.E.; Niemann, C.U. Clinical Outcomes in Patients with Multi-Hit TP53 Chronic Lymphocytic Leukemia Treated with Ibrutinib. *Clin. Cancer Res.* **2021**, *27*, 4531–4538. [CrossRef]
156. Fornalski, K.W.; Dobrzyński, L. Modeling of single cell cancer transformation using phase transition theory: Application of the Avrami equation. *Radiat. Environ. Biophys.* **2022**, *61*, 169–175. [CrossRef]
157. Mitchell, S.R.; Gopakumar, J.; Jaiswal, S. Insights into clonal hematopoiesis and its relation to cancer risk. *Curr. Opin. Genet. Dev.* **2021**, *66*, 63–69. [CrossRef]
158. Tang, S.; Lu, Y.; Zhang, P.; Chen, D.; Liu, X.; Du, X.; Cao, J.; Ye, P.; Chen, L.; Li, S.; et al. Lenalidomide, bortezomib and dexamethasone followed by tandem-autologous stem cell transplantation is an effective treatment modality for multi-hit multiple myeloma. *Leuk. Res.* **2021**, *110*, 106710. [CrossRef]
159. Reece, A.S.; Hulse, G.K. A geospatiotemporal and causal inference epidemiological exploration of substance and cannabinoid exposure as drivers of rising US pediatric cancer rates. *BMC Cancer* **2021**, *21*, 197–230. [CrossRef] [PubMed]